Locally Range-Separated Local Hybrid Functionals – The Next Level on the Hybrid Functional Ladder

Toni M. Maier[a)]
Technische Universität Braunschweig, Institut für Physikalische und Theoretische Chemie, Gaussstraße 17, D-38106 Braunschweig, Germany

(Dated: 24 March 2023)

In this work, the new class of locally range-separated local hybrid (LRSLH) functionals is presented. LRSLH functionals combine the concepts of a local exact-exchange admixture as in local hybrids with a locally range-separated exact-exchange admixture as in locally range-separated hybrid functionals. The satisfiability of important theoretical constraints on hybrid functionals by the LRSLH approach is discussed in comparison to existing hybrid functional classes by proposing a new categorization scheme for hybrid functionals, labeled as hybrid functional ladder. In particular, this concerns the iso-orbital and asymptotic potential limits as well as the high-density limit with respect to uniform coordinate scaling and the gradient expansion of the exchange energy density, which in contrast to existing hybrid schemes can be simultaneously satisfied by LRSLH functionals. Furthermore, this work provides a first explorative study regarding the performance of the new LRSLH approach. Despite featuring only up to two empirical parameters, the optimized LRSLH functionals exhibit a similar performance for atomization energies and transition barrier heights as some of the more recent hybrid functionals. In particular, this highlights the great potential of the new LRSLH approach.

Keywords: Density Functional Theory, Exchange-Correlation Functionals, Hybrid Functionals, Local Hybrid Functionals, Local Range Separation

I. INTRODUCTION

Owing to its often excellent ratio between the achievable accuracy and the required computation costs, hybrid functionals, which have been first developed by Becke in 1993 based on an adiabatic connection formalism,[1] have evolved into one of the most popular and successful classes of exchange-correlation (XC) functionals within density functional theory (DFT) thus far.[2–6] In particular, by replacing a certain amount of (semi-)local exchange by Hartree-Fock-like exact exchange, the self-interaction error (SIE)[7] inherent to (semi-)local exchange functionals is mitigated. While employing 100% exact exchange would fully cancel the SIE, it is known that (semi-)local exchange implicitly describes non-local correlation effects.[8] Conventional hybrid functionals are thus a compromise between the necessity to accurately describe correlation effects and cancelling the SIE and as such generally aim to balance out both effects.[9] Hence, for a wide range of different properties, ranging from themochemistry to transition barrier heights[10] to excitation energies,[11] hybrid functionals are able to provide higher accuracies than Hartree-Fock and conventional semi-local XC functionals, while formally exhibiting similar computational costs. The most simple approach to incorporate an exact-exchange admixture, which has been proposed in the initial work by Becke,[1] is to introduce a simple mixing constant $0 < a \leq 1$, yielding the global hybrid (GH) exchange energy functional

$$E_{\mathrm{x},\sigma}^{\mathrm{gh}} = a \cdot E_{\mathrm{x},\sigma}^{\mathrm{ex}} + (1-a) \cdot E_{\mathrm{x},\sigma}^{\mathrm{sl}} \,, \tag{1}$$

where $E_{\mathrm{x},\sigma}^{\mathrm{ex}}$ and $E_{\mathrm{x},\sigma}^{\mathrm{sl}}$ are the exact-exchange and semi-local exchange energies, respectively. During the last decades, a large variety of different global hybrid models have been developed,[12–14] e.g., by employing more sophisticated approaches for the semi-local exchange energy tuned for being used in combination with exact exchange.[15] While the best performing global hybrids are often able to provide accuracies close to more sophisticated electronic structure methods,[16–18] global hybrids in general still suffer from several systematic shortcomings. First of all, the optimal global mixing constant a has been found to vary significantly for different properties. While molecular structures are often already well described with small a,[19,20] moderate values of a around 0.20 to 0.25 as in B3LYP[13] and PBE0[12] generally perform well for thermochemistry.[10,18] However, higher values are usually needed to accurately describe transition barrier heights[10,21,22] as well as core, Rydberg and long-range charge-transfer excitations calculated with linear-response time-dependant DFT.[11,23–29] In fact, the latter properties are prominent cases in which conventional global hybrid functionals with a medium amount of exact exchange are known to fail systematically. Furthermore, global hybrids, as the underlying semi-local XC functionals and Hartree-Fock, are not able to describe non-local long-range correlation effects such as dispersion, thus usually requiring either a dedicated non-local correlation functional such as VV10,[30] local dispersion models,[31,32] a force-field-like correction as in D3 or D4[33–35] or similar models.[36] Similarly, conventional global hybrids cannot describe strong correlation effects, except dedicated non-local strong-correlation models are incorporated[37–40] or schemes beyond the usually applied GKS scheme[41] are used.[42]

In range-separated hybrid (RSH) functionals,[25,43–50] the exchange functional is separated into a long- and a short-range part based on a range-separation of the underlying Coulomb operator with respect to the inter-electronic distance, usually by combining either an error or erfgau function[51] with a positive constant range-separation parameter. In its most common scheme, RSH functionals combine long-range exact exchange $E_{\mathrm{x},\sigma}^{\mathrm{ex,lr}}$ with a short-range semi-local exchange functional $E_{\mathrm{x},\sigma}^{\mathrm{sl,sr}}$

$$E_{\mathrm{x},\sigma}^{\mathrm{rsh}} = E_{\mathrm{x},\sigma}^{\mathrm{ex,lr}} + E_{\mathrm{x},\sigma}^{\mathrm{sl,sr}} \,, \tag{2}$$

which in contrast to global hybrids with $a < 1$, is able to provide the correct asymptotic exchange potential.[25] In fact, the latter has been found to be crucial for the accurate descrip-

a)Electronic mail: toni.maier@tu-braunschweig.de; ORCiD: 0000-0001-5571-7576

tion of long-range excitations in linear-response TDDFT, such as many charge-transfer and some Rydberg excitations[11,25,52] and thus effectively eliminates one of the systemic shortcomings of global hybrid functionals. On the other hand, RSHs using exact exchange in the short-range[53] have been found to be generally beneficial for the description of core excitations with linear-response TDDFT.[52] However, as for global hybrids a reparametrization for elements in different periods is required. While only a few functionals feature a combination of short- and long-range exact exchange,[52,54,55] most modern RSH approaches such as the ωB97X family[56–58] or CAM-B3LYP[59] combine long-range exact exchange with a global-hybrid-like exact-exchange admixture. Accordingly, these RSHs are often able to provide accurate CT excitations while to a large extend retaining the accuracy of global hybrids for many ground-state properties.

However, as for global hybrid functionals, the constant range-separation parameter in conventional RSH functionals has been found to significantly depend on the investigated system and excitation.[60,61] This has led to a number of different optimal tuning approaches,[62–66] which, despite improving calculated excitation spectra, violate size consistency by construction and as such are applicable only for specialized problems. Another more sophisticated approach, that introduces a system-dependency into RSH functionals while retaining size-consistency, are locally range-separated hybrid (LRSH) functionals, which have been introduced by Savin and coworkers in 2008.[67] In particular, the range separation constant in conventional RSHs is replaced by a real-space-dependent range-separation function (RSF), thus being able to adapt the range separation depending on the molecular environment. Mostly due to recent advancements in semi-numerical integration techniques, which enable an efficient calculation of the occuring non-standard exact-exchange integrals,[68] LRSH functionals have gained more attention just recently.[69,70] In particular, this concerns the development of new models for the RSF. For example, this includes the recent models by Kümmel and co-workers[71,72] as well as a non-empirical scheme to derive RSFs from satisfying the gradient expansion of the exchange hole to a certain order.[73] However, LRSH functionals are still in an early development phase compared to the other hybrid functional approaches, with the satisfiability of exact constraints such as the high-density limit with respect to homogeneous coordinate scaling and the iso-orbital constraint still being discussed.[72,73]

In a similar way as in the LRSH approach, the global mixing constant in global hybrid functionals can be replaced by a real-space-dependent local mixing function (LMF), yielding so-called local hybrid (LH) functionals, introduced twenty years ago by Jaramillo *et al.*[74] Apart from providing a more flexible exact-exchange admixture than in global hybrids by being able to adapt to the molecular environment, introducing a real-space dependence through the LMF allows the satisfaction of a number of additional physical constraint compared to global hybrids, including, e.g., the iso-orbital limit[74] and the high-density limit with respect to uniform coordinate scaling.[75] On the other hand, the LH approach requires the calculation of non-standard exact-exchange integrals similar to the LRSH scheme and suffers from the so-called gauge problem due to the admixture of exchange energy densities rather than exchange energies.[76] In fact, these problems have been solved effectively by employing efficient semi-numerical integration schemes[19,77–84] and the introduction of suitable calibration function (CF) models,[85–87] respectively. Accordingly, the development of more physical and accurate LMF models is in the focus of current local hybrid research. However, despite several attempts, more sophisticated LMF approaches[75,88–92] did not provide significant improvements compared to the simple t-LMF,[93,94] which is the most successful LMF thus far. Nonetheless, recently developed t-LMF-based LH functionals such as LH20t[9] have already shown great potential in simultaneously describing ground state thermochemistry and different electronic excitation classes with high accuracy.[23] In fact, local hybrids in general have been shown to be able to systematically solve the problem of accurately describing core and Rydberg excitations,[23] which is usually not possible with conventional RSHs. However, local hybrids are not able to provide the correct asymptotic XC potential[95] and thus accurate long-range charge-transfer excitations.[23] More recent developments include the combination of local hybrids with conventional range-separated hybrid functionals (range-separate local hybrids, RSLHs)[96,97] as well as efforts to mimic strong correlation effects[98,99] similar to the B05 family of functionals,[37,38] which essentially can be viewed as a special form of local hybrid functionals. A more comprehensive summary of local hybrids can be found in a recent review.[100]

While the more recent hybrid functional approaches individually are thus able to solve many of the main issues of conventional global hybrid functionals, currently none of them is able to do so simultaneously. For example, the iso-orbital limit and the correct uniform coordinate scaling in the high-density limit in principle can be satisfied by local hybrid functionals, while it is not possible to provide the correct asymptotic exchange potential. On the other hand, the latter can be easily implemented using LRSH functionals, while the reasonability satisfying the former two constraints within the LRSH approach is still debated. The most straightforward approach to enable simultaneous satisfaction of all these constraints, which is presented in this work but has not been investigated thus far, is the unification of the LH and LRSH approaches within a common hybrid functional class, which will be called locally range-separated local hybrid (LRSLH) functionals.

The present work is structured as follows. First, the theoretical background of the new LRSLH approach will be described in detail in sec. II. Apart from their formal mathematical description, this includes the embedding of the LRSLH model into a new general ordering scheme for hybrid functionals similar to the prominent Jacob's Ladder of XC functional approximations[101] as well as a detailed discussion of satisfiable theoretical constraints within this new ordering scheme. Following this, the performance and benefits of the new LRSLH approach will be examined in comparison to the other hybrid functional classes by optimizing and evaluating various hybrid functional models with respect to conventional thermochemical and transition barrier height test sets. While the investigated functional models and computational details are described in detail in secs. III and IV, respectively, the results of this explorative study are discussed in sec. V.

II. THEORY

A. Locally Range-Separated Local Hybrid Functionals

In the following, the underlying mathematical background of the new LRSLH model will be described in detail. Here, μ, ν have been used as general basis function indices and $\sigma, \varsigma \in \{\alpha, \beta\}$ as spin indices. For clarity, the space variable $\mathbf{r}$ will be omitted, except in cases in which it is considered essential for understanding.

Being a combination of LH and LRSH functionals, the LRSLH exchange energy functional in its spin-resolved form can be expressed as

$$E_{\mathrm{x},\sigma}^{\mathrm{lrslh}} = \int g_\sigma \cdot e_{\mathrm{x},\sigma}^{\mathrm{ex}} \,\mathrm{d}\mathbf{r} + \int [1 - g_\sigma] \cdot \left[e_{\mathrm{x},\sigma}^{\mathrm{lrsh}} + G_\sigma\right] \mathrm{d}\mathbf{r} \,, \quad (3)$$

where g_σ is the local mixing function (LMF) managing the real-space-dependent admixture of the full-range exact-exchange energy density

$$e_{\mathrm{x},\sigma}^{\mathrm{ex}}(\mathbf{r}) = -\frac{1}{2} \cdot \mathbf{X}^{\mathrm{T}} \mathbf{D}^\sigma \mathbf{A}^\sigma \mathbf{D}^\sigma \mathbf{X} \quad (4)$$

to the LRSH exchange energy density $e_{\mathrm{x},\sigma}^{\mathrm{lrsh}}$. $\mathbf{X}$ denotes the basis function vector at the position $\mathbf{r}$ within the basis $\{\chi_\mu\}$, $\mathbf{D}^\sigma$ the corresponding spin density matrices and

$$A_{\mu\nu}^\sigma(\mathbf{r}) = \int \frac{\chi_\mu(\mathbf{r}')\,\chi_\nu(\mathbf{r}')}{|\mathbf{r} - \mathbf{r}'|} \mathrm{d}\mathbf{r}' \,. \quad (5)$$

the associated real-space-dependent two-center integrals over the Coulomb operator, commonly denoted as $\mathbf{A}$ matrix. In the same way as local hybrids,[76,85,86] LRSLH functionals suffer from the so-called gauge problem caused by the local admixture of exchange energy densities. In particular, exchange energy densities as $e_{\mathrm{x},\sigma}^{\mathrm{ex}}$ and $e_{\mathrm{x},\sigma}^{\mathrm{lrsh}}$ are only defined up to a function integrating to a vanishing contribution in the exchange energy. Hence, adding a so-called calibration function (CF) G_σ with

$$\int G_\sigma(\mathbf{r}) \,\mathrm{d}\mathbf{r} = 0 \quad (6)$$

to either of the two exchange energy densities to consider the potential mismatch between their gauge origins is necessary. While introducing a CF has no effect on GH and RSH functionals, a local admixture as in LH and LRSLH functionals gives the additional non-vanishing energy term

$$\int g_\sigma \cdot G_\sigma(\mathbf{r}) \,\mathrm{d}\mathbf{r} \neq 0 \,. \quad (7)$$

For local hybrids, it is known that neglecting the gauge problem, i.e., setting $G_\sigma = 0$, can cause some issues, e.g., too repulsive dissociation curves of noble gas dimers[86] or unreasonable empirical dispersion corrections.[102] Therefore, a number of different approaches for constructing suitable CF models have been proposed,[86,87] with CFs based on the pig scheme[85] being the currently best compromise between computational costs and effectiveness regarding the mitigation of the mentioned issues.

While in principle $e_{\mathrm{x},\sigma}^{\mathrm{lrsh}}$ can be any locally range-separated exchange energy density, i.e., featuring short- or long-range exact exchange as well as combinations of both, the formalism will be explained here only for the most common case of long-range exact exchange. In this case,

$$e_{\mathrm{x},\sigma}^{\mathrm{lrsh}} = e_{\mathrm{x},\sigma}^{\mathrm{ex,lr}} + e_{\mathrm{x},\sigma}^{\mathrm{sl,sr}} \,, \quad (8)$$

with the long- and short-range parts of the underlying Coulomb operator being given by

$$\frac{1}{|\mathbf{r} - \mathbf{r}'|} = \frac{\mathrm{erf}\left(\omega_\sigma \cdot |\mathbf{r} - \mathbf{r}'|\right)}{|\mathbf{r} - \mathbf{r}'|} + \frac{1 - \mathrm{erf}\left(\omega_\sigma \cdot |\mathbf{r} - \mathbf{r}'|\right)}{|\mathbf{r} - \mathbf{r}'|} \,, \quad (9)$$

where ω_σ is the real-space-dependent range separation function (RSF). While a range-separation based on the erfgau or a Gaussian function are also possible in principle,[51] only the most common case of an error function will be considered here. Accordingly, the long-range exact-exchange energy density is given by

$$e_{\mathrm{x},\sigma}^{\mathrm{ex,lr}} = -\frac{1}{2} \cdot \mathbf{X}^{\mathrm{T}} \mathbf{D}^\sigma \mathbf{A}^{\sigma,\mathrm{lr}} \mathbf{D}^\sigma \mathbf{X} \quad (10)$$

with the long-range $\mathbf{A}$ matrix

$$A_{\mu\nu}^{\sigma,\mathrm{lr}}(\mathbf{r}) = \int \mathrm{erf}\left(\omega_\sigma \cdot |\mathbf{r} - \mathbf{r}'|\right) \cdot \frac{\chi_\mu(\mathbf{r}')\,\chi_\nu(\mathbf{r}')}{|\mathbf{r} - \mathbf{r}'|} \mathrm{d}\mathbf{r}' \,. \quad (11)$$

On the other hand, an exact formula for the short-range (semi-)local exchange energy density $e_{\mathrm{x},\sigma}^{\mathrm{sl,sr}}$ is only known for Slater-Dirac exchange,[103,104] i.e., within the local density approximation (LDA). For short-range exchange functionals on the generalized-gradient approximation (GGA) level, different approximations have been proposed.[105,106] One of the most common ones is the one by Hirao and co-workers,[43] which is used throughout this work, as in contrast to some other approaches it provides the correct LDA limit. $e_{\mathrm{x},\sigma}^{\mathrm{sl,sr}}$ is then given by

$$e_{\mathrm{x},\sigma}^{\mathrm{sl,sr}} = -\frac{3}{2}\left(\frac{3}{4\pi}\right)^{1/3} \rho_\sigma^{4/3} \cdot [1 + F_\sigma^{\mathrm{x}}] \cdot [1 - f_\sigma] \,, \quad (12)$$

where f_σ is the long-range separation factor within the Hirao approach

$$f_\sigma = \frac{8}{3} a_\sigma \left[\sqrt{\pi} \cdot \mathrm{erf}\left(\frac{1}{2a_\sigma}\right) - 3a_\sigma + 4a_\sigma^3 + \left(2a_\sigma - 4a_\sigma^3\right) \cdot \exp\left(-\frac{1}{4a_\sigma^2}\right)\right] \quad (13)$$

with the auxiliary quantity

$$a_\sigma = \frac{1}{k} \cdot \frac{\omega_\sigma}{\rho_\sigma^{1/3}} \cdot \sqrt{1 + F_\sigma^{\mathrm{x}}} \,, \quad (14)$$

the electron spin density ρ_σ, the GGA enhancement factor F_σ^{x} and $k = 2\left(6\pi^2\right)^{1/3}$.

Eq. (3) is the common expression of the LRSLH approach within the *exchange picture*,[73] highlighting the interpretation of LRSLH exchange as exchange functional. However, as possible for all hybrid functionals, one can recast eq. (3) in such a way that LRSLH exchange gives an energy correction to the exact-exchange energy $E_{\mathrm{x}}^{\mathrm{ex}}$, yielding the LRSLH XC energy functional

$$E_{\mathrm{xc}}^{\mathrm{lrslh}} = E_{\mathrm{x}}^{\mathrm{ex}} + E_{\mathrm{nlc}}^{\mathrm{lrslh}} + E_{\mathrm{c}}^{\mathrm{sl}} \quad (15)$$

$$E_{\mathrm{nlc}}^{\mathrm{lrslh}} = \sum_\sigma \int [1 - g_\sigma] \cdot \left[e_{\mathrm{x},\sigma}^{\mathrm{sl,sr}} - e_{\mathrm{x},\sigma}^{\mathrm{ex,sr}} + G_\sigma\right] \mathrm{d}\mathbf{r} \,. \quad (16)$$

That is, in addition to the semi-local correlation functional E_c^{sl}, the LRSLH approch provides the additional non-local correlation term E_{nlc}^{lrslh}. Since E_c^{sl} usually covers most dynamical correlation effects, E_{nlc}^{lrslh} is formally often interpreted as non-dynamical correlation in the context of local hybrid functionals.[100] While this formal *ansatz* has been successfully used to mimic non-dynamical correlation effects to some extent, e.g., in more recent functionals by the Kaupp group[98,99] or implicitly in the B05 family of functionals,[37,38] KP16[39] or the DM21 functional,[107] it should be noted that the alternative interpretation as non-local dynamical correlation functional is equally justified but has not been explicitly employed thus far. Either way, the reformulation of the LRSLH approach into the *correlation picture* provides an additional angle on the LRSLH model to exploit theoretical constraints (see sec. II C for details).

As for the underlying LH and LRSH functionals, the occurring non-standard exact-exchange integrals in LRSLH functionals and their Fock matrix elements

$$\mathbf{F}_{xc,\sigma}^{lrslh} = \frac{\partial E_{xc}^{lrslh}}{\partial \mathbf{D}^{\sigma}} , \tag{17}$$

which are required for a self-consistent implementation, and higher derivatives cannot be calculated analytically. However, the occurring non-standard exact-exchange integrals are identical to the ones in the LH and LRSH approaches. Explicit expressions for the Fock matrix elements for the latter two can be found in refs. 100 and 73. Hence, the implementation of LRSLH functionals into quantum chemistry codes that already feature LH and LRSH functionals, such as Turbomole[108] or Raqet,[109] is rather straightforward. In particular, this enables reusing already existing implementations of efficient semi-numerical integration schemes such as the modified COSX method.[77] Accordingly, computation costs of LRSLH functionals are comparable to those of LRSH functionals with a global exact exchange component.

B. Hybrid Functional Ladder

During the last decades a myriad of different approximations to the XC functional have been developed. The first and most popular scheme to categorize different approximations is the so-called Jacob's Ladder of XC approximations, introduced by Perdew and Schmidt in 2001.[101] In particular, their scheme distinguishes between five different rungs of ascending complexity, the LDA, the GGA, the meta-GGA, the hyper-GGA and the generalized random-phase approximation. To consider functionals featuring just a linear dependence on the non-local density matrix explicitly, Janesko has extended the original scheme by rung 3.5 functionals.[110] While the former three rungs, which are often grouped together as (semi-)local functionals, mainly differ in the employed local ingredients and applicable theoretical constraints, from a technical and performance point of view they are often rather similar. On the other hand, all the different hybrid functional classes are grouped together with other non-local occupied-orbital-dependent functionals such as UW12[111,112] within the hyper-GGA rung, despite enabling the satisfaction of different theoretical constraints, featuring different ingredients and required integration techniques and providing different systematic shortcomings for the calculation of various properties. In fact, since most of the newly developed XC functionals contains a certain amount of exact exchange in one or the other way, they can be formally identified as hyper-GGA or hybrid functionals. However, this does not necessarily suffice to fully characterize the general features of the functional. While different hybrid functional classes have been introduced during the last decades, a more detailed systematic categorization scheme for different hybrid functionals would be beneficial.

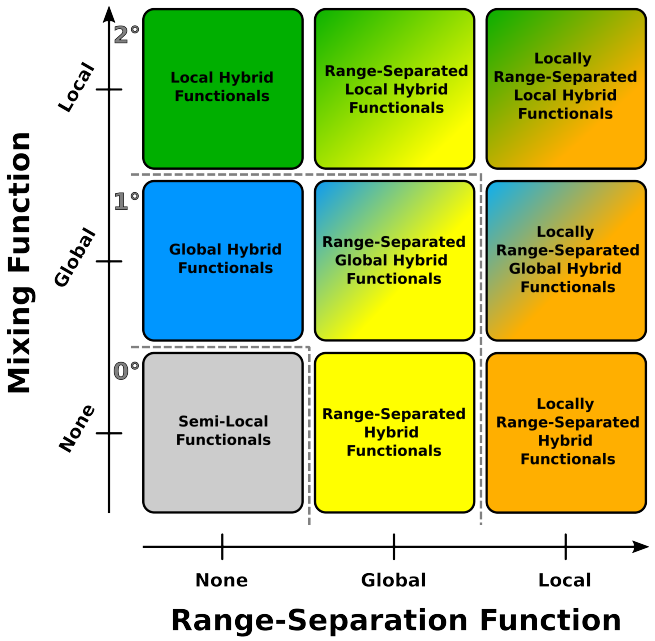

FIG. 1. Graphical representation of the hybrid functional ladder up to second order.

In analogy to the Jacob's Ladder by Perdew and Schmidt,[101] I thus propose a new hybrid functional ladder for ordering the different known hybrid functional classes with respect to their complexity and the required computational efforts, including the new LRSLH functionals. A graphic representation can be found in fig. 1. In particular, two independent ordering parameters are considered, the RSF and the mixing function, as described in detail in sec. II A within the context of the LRSLH approach. In fact, in the case neither a mixing function nor an RSF is used, i.e., $g_\sigma = 0$ and $\omega_\sigma = 0$, one obtaines a pure semi-local (SL) exchange functional. While this is no real hybrid functional, it can be interpreted as a 0th order hybrid or as 0th rung, similar to the Hartree world in the original scheme. Obviously, no exact-exchange integrals need to be calculated on the 0th rung. Alternative choices for the RSF and the mixing function are a) a global constant, b) a local function depending on $\mathbf{r}$ and c) a non-local function depending on the two independent space variables $\mathbf{r}$ and $\mathbf{r}'$. A graphical representation of the amount of exact exchange admixed in the different classes of the hybrid functional ladder is given in fig. 2 to highlight their differing complexity.

Hybrid functionals containing at most a non-vanishing constant for the RSF or the mixing function are categorized as first order functionals. This includes global hybrids ($g_\sigma = \text{const.} \neq 0$, $\omega_\sigma = 0$) and RSH functionals ($g_\sigma = 0$, $\omega_\sigma = \text{const.} \neq 0$). In fact, many functionals usually identi-

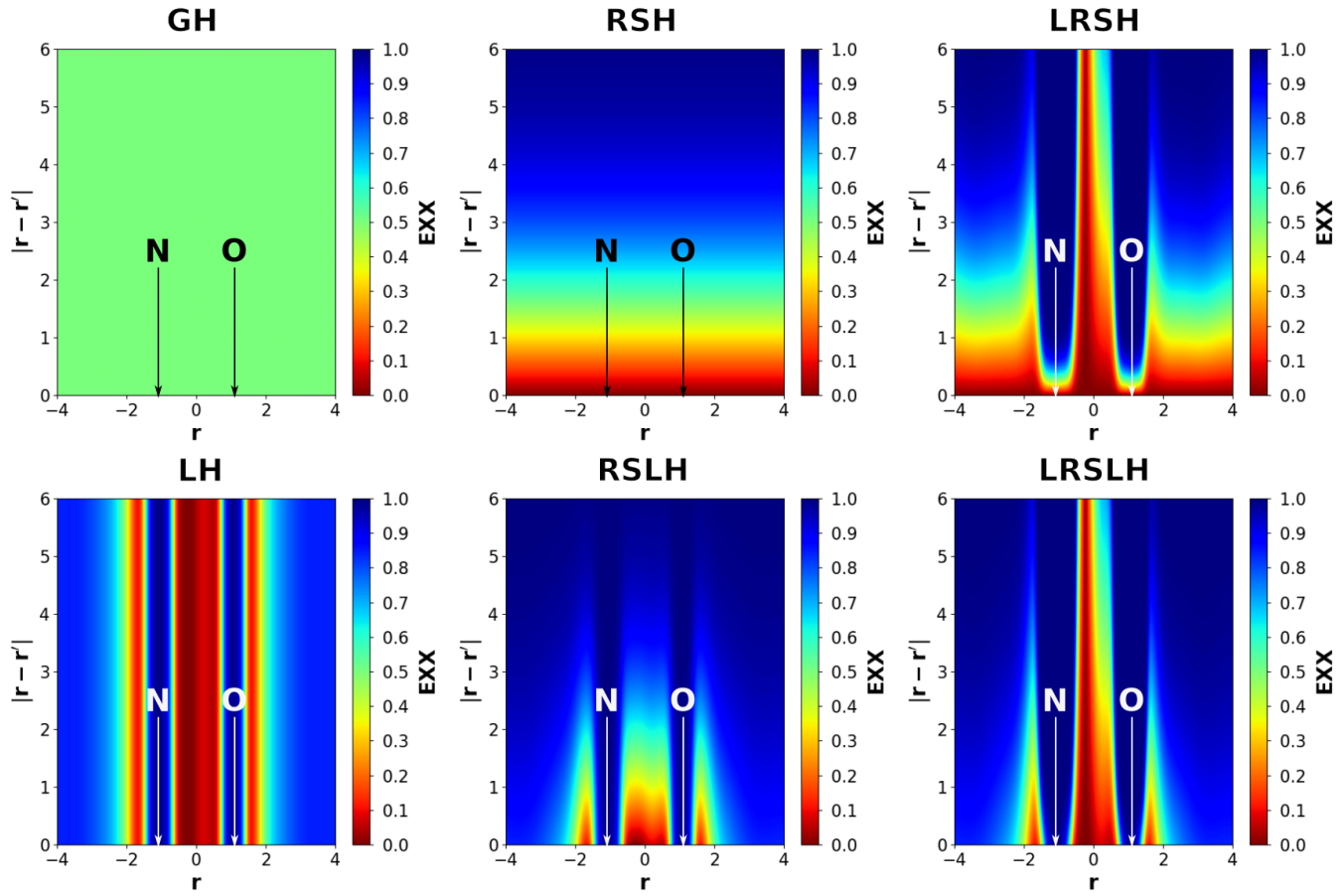

FIG. 2. Exact exchange (EXX) admixture depending on the inter-electronic distance $|\mathbf{r}-\mathbf{r}'|$ and the real-space coordinate $\mathbf{r}$ along the bonding axis of the NO molecule within six different hybrid functional classes. A mixing constant of $a = 0.5$, an unscaled common t-LMF, a constant range separation parameter $\omega_\sigma = 0.3\ a_0^{-1}$ and an unscaled ge2-RSF have been used for the plots.

fied as range-separated hybrids such as ωB97X-D[57] do not fall in either of both categories. Instead they would be categorized as range-separated global hybrid (RSGH) functionals due to the incorporation of a constant amount of exact exchange in the short range. Since pure RSHs as LC-BLYP[60] often exhibit a significantly different performance than range-separated global hybrids, this distinction appears to be reasonable. RSGH functionals, which include many of the currently most accurate hybrid functionals, thus provide the most complexity of the three subclasses on the first rung of the hybrid functional ladder. Regarding the calculation of the exact-exchange integrals, analytical integration schemes can be employed (although semi-numerical methods might be advantageous).

On the second rung, the mixing function and the RSF are allowed to exhibit a real-space dependence. Apart from the already investigated classes, i.e., LHs ($g_\sigma(\mathbf{r})$, $\omega_\sigma = 0$), LRSHs ($g_\sigma = 0$, $\omega_\sigma(\mathbf{r})$) and RSLHs ($g_\sigma(\mathbf{r})$, $\omega_\sigma = \text{const.} \neq 0$), this also includes locally range-separated global hybrid (LRSGH) functionals ($g_\sigma = \text{const.} \neq 0$, $\omega_\sigma(\mathbf{r})$) and the new class of LRSLH functionals ($g_\sigma(\mathbf{r})$, $\omega_\sigma(\mathbf{r})$). In fact, the new LRSLH approach is the most sophisticated of the second-rung hybrid functional schemes, as it unifies the concepts of all other subclasses on the second rung of the hybrid functional ladder. As such, the introduction of LRSLH functionals closes a missing gap within this scheme and all other hybrid functional classes up to the second rung can be viewed as special cases of LRSLH functionals. In contrast to hybrid functionals on the first rung, exact-exchange integrals cannot be calculated analytically but require a semi-numerical integration in one or the other way.

On the third rung, which is not shown explicitly in fig. 1, the mixing function and the RSF are allowed to become non-local themselves, thus formally yielding non-local hybrid, range-separated non-local hybrid, locally range-separated non-local hybrid, non-locally range-separated hybrid, non-locally range-separated global hybrid, non-locally range-separated local hybrid and non-locally range-separated non-local hybrid functionals, with the latter providing the most flexibility for third-rung hybrid functionals. However, to my best knowledge none of the current XC functional approximations can be categorized into the third rung. One of the main reasons for that might be that occurring non-standard exact-exchange integrals in general would need to be calculated fully numerically, i.e., employing a double-grid integration as in VV10. Apart from potential efficiency problems, the Coulomb cusp might be one concern regarding numerical stability. Furthermore, a full numerical double-grid integration would already enable calculations with all kinds of other hyper-GGA functionals. Hence, the restriction to just

non-local-hybrid-like functionals is an unnecessary restriction from a technical point of view. Accordingly, while a third rung on the hybrid functional ladder can be proposed formally, its usefulness in practice is questionable.

C. Theoretical Constraints

In the history of XC functional development, theoretical constraints have played a major role for many new developments and often were the driving force to improve existing XC functionals.[113,114] Even modern machine-learning approaches often heavily rely on exact theoretical constraints rather than just a large number of reference data.[107] When ascending the Jacob's Ladder of density functional approximations, an additional set of constraints can be satisfied on each rung. For example, GGA functionals can give the correct gradient expansion of the exchange energy density[115] and the exchange potential, but cannot do so simultaneously.[116,117] On the meta-GGA level, the SCAN functional and its successors[118,119] aim to satisfy all constraints satisfiable by third-rung functionals. Similarly, a number theoretical constraints for functionals on the fourth rung of Jacob's Ladder are known and are used across the literature mainly for the construction of hybrid functionals.[75,100]

In this work, those theoretical constraints that are directly related to the exact-exchange admixture will be reviewed in view of the various hybrid functional classes. Hence, the considered constraints are just a subset of constraints that can be considered to be important in the context of hybrid functionals. In particular, this includes the iso-orbital limit, the behavior under uniform coordinate scaling, the asymptotic XC potential and the homogeneous limit and gradient expansion of the exchange energy density. Theoretical constraints such as the Lieb-Oxford bound,[90,120,121] the flat-plane condition[6,107,122] and satisfaction of the IP theorem[61] have been shown to be satisfiable within certain hybrid setups but provide more indirect information about the exact-exchange admixture. Theoretical constraints on the exact XC functional that target strong correlation effects, such as the correct behavior upon closed-shell bond-breaking, are intentionally excluded from the discussion to circumvent necessary assumptions regarding the interpretation of the additional non-local correlation term eq. (16) as non-dynamical correlation, since this would go beyond the scope of the present work.

In the following, the four mentioned theoretical constraints will be described in more detail and the satisfiability within the different hybrid functional classes will be assessed. The results are summarized in table I. In this respect it should be noted that Hartree-Fock satisfies all of these constraints by default. Accordingly, the Hartree-Fock limit is excluded from the consideration, if it could be constructed within a certain hybrid functional class, e.g., RSHs with an infinite ω.

TABLE I. Satisfiability of theoretical constraints by the different hybrid functional classes. −, (+) and + means not satisfiable, satisfiable with restrictions and fully satisfiable, respectively.

Class	Constraint			
	Iso-Orbital	HDL[a]	Asymp. Pot.[b]	Hom. Limit[c]
SL	−	−	−	+
GH	−	−	−	+
RSH	−	−	+	−
RSGH	−	−	+	−
LRSH	(+)	(+)	+	+
LRSGH	(+)	(+)	+	+
LH	+	+	−	+
RSLH	+	+	+	−
LRSLH	+	+	+	+

[a] High-density limit with respect to homogeneous coordinate scaling
[b] Asymptotic exchange potential.
[c] Homogeneous limit and gradient expansion of exchange energy density.

1. Iso-Orbital Limit

The iso-orbital limit or iso-orbital constraint concerns regions in real space, which exclusively feature a single occupied orbital.[74,100,123,124] In these iso-orbital regions, the probability to find two electrons with same spin at the same position $\mathbf{r}$ is exactly 0. Accordingly, same-spin correlation contributions are absent, so the self-interaction error (SIE) of the classical Coulomb interaction, which is a same-spin contribution, needs to be cancelled fully by employing 100% exact exchange. A special case of iso-orbital regions are iso-electron regions.[125] In particular, iso-electron regions feature the additional constraint that the probability to find two electrons with opposite spin at the same position $\mathbf{r}$ is also exactly 0, while it can be generally non-zero in iso-orbital regions. That is, opposite-spin correlation, which in general can occur in iso-orbital regions if the single spatial orbital is doubly occupied, is absent in iso-electron regions. Imposing 100% exact exchange only in iso-electron regions, but not in iso-orbital regions in general, is referred to as iso-electron limit or iso-electron constraint. The iso-electron limit is automatically satisfied if the iso-orbital limit is satisfied, but not vice versa, so the iso-orbital limit is the stronger constraint.

In fact, satisfying the iso-orbital limit by hybrid functionals has the consequence that the remaining opposite-spin correlation in two-electron iso-orbital systems such as H_2 and the helium atom is required to be fully described by an additional dedicated correlation functional, since eq. (16) is constrained to give a vanishing non-local correlation contribution. That is, the iso-orbital constraint imposes a vanishing same-spin correlation contribution from hybrid exchange in two-electron iso-orbital systems. In contrast, just imposing the iso-electron limit does not impose any constraints on two-electron iso-orbital systems. Accordingly, eq. (16) is allowed to give a non-vanishing correlation contribution for two-electron iso-orbital systems, i.e., the opposite-spin correlation at least in parts can be described by the exchange functional. In fact, the latter is implicitly exploited as part of the systematic error compensation in most semi-local and hybrid XC functionals.[8] In particular, this concerns the balance between the semi-local correlation hole and the non-local hole stemming from eq. (16) to approximate the exact correlation hole.[4] However, relying on this systematic error compensation is known to play a major role in the zero-sum tradeoff problem of GH functionals between the performance for different properties and thus is one of the major aspects limiting the accuracy achievable with

conventional GH functionals. As pointed out, e.g, by Janesko on the example of LH functionals,[4] one of the main goals of more sophisticated hybrid functional schemes such as LRSH and LRSLH functionals is, however, to achieve beyond-zero-sum accuracies. Intrinsically, this goes along with replacing the systematic error compensation from GH functionals with more accurate correlation functionals. In this sense, it appears more reasonable to require new hybrid functionals to satisfy the stronger iso-orbital limit instead of the iso-electron constraint, since the latter imposes no restrictions needed to prevent the outlined error compensation effects in closed-shell systems.

While exact iso-orbital regions occur only in a few systems as those mentioned above, satisfaction of the iso-orbital constraint can be important in many more cases, in particular, in regions that are dominated by just one occupied orbital and thus can be identified as effective iso-orbital regions. In molecular systems, this concerns mainly two different cases, regions far away from the molecule, which will be denoted as *asymptotic regions* and should not be confused with the asymptotic behavior in inter-electronic space, and regions close to the nuclei.[100] In asymptotic regions, the electron density is dominated by that occupied orbital with the slowest exponential decay. While the contribution from the other occupied orbitals is not exactly 0, their influence diminishes exponentially when going farther away from the molecule. Hence, asymptotic regions can be identified as effective iso-orbital regions. In the context of LH functionals, it has been found that the intermediate regions between valence and asymptotic regions are responsible for the accurate description of Rydberg excitations,[23] so satisfying the iso-orbital constraint in asymptotic regions is an important limiting case.

Similarly, the respective 1s orbitals dominate the electron density at the nuclei. While higher angular momentum orbitals at the same nucleus exhibit nodes and thus vanish exactly, the contribution from orbitals of other nuclei is negligible. That is, only s orbitals contribute to the electron density at a respective nucleus, with the 1s orbital obviously having by far the largest contribution. While this effect becomes more pronounced for heavy elements, contributions from higher s orbitals might still have a significant contribution for light elements. Hence, nuclei positions can be identified in most parts as effective iso-orbital regions, in particular, for heavier elements, while lighter elements might still feature a slight multi-orbital character. Satisfying the iso-orbital limit at the nuclei positions is obviously relevant for the accurate description of core excitations using linear-response TDDFT, which cannot be achieved by just satisfying the iso-electron limit.

Regarding the different hybrid functional classes, the identification of iso-orbital regions requires a real-space-dependent exact-exchange admixture. While this is obviously provided by the LH, RSLH and LRSLH approaches through the LMF, the RSF in LRSH and LRSGH functionals in principle can also be used to identify iso-orbital regions. However, satisfying the iso-orbital limit in the latter two approaches requires to implement a pole into the RSF,[72] which is not compatible with the constraint to satisfy the second-order gradient expansion with the locally range-separated exchange energy density (see sec. II C 4 for more details).[73] While in the new LRSLH model the iso-orbital limit in principle could be satisfied either by a suitable LMF and the RSF, it is thus most reasonable to assign the iso-orbital limit as an exact constraint to the LMF to avoid incompatibilities with the gradient expansion constraint.

2. Uniform Coordinate Scaling

The second considered constraint for hybrid functionals is their behavior under uniform coordinate scaling, which is a powerful theoretical concept, in which the scaled space variable $\mathbf{r} \to \mathbf{r}_\lambda = \lambda\mathbf{r}$ with the scaling parameter $0 \leq \lambda \leq \infty$ is introduced. In the most common approach,[126–128] the total electron number is kept fixed, which results in a scaling of the electron density of

$$\rho_\sigma(\mathbf{r}) \to \lambda^3 \cdot \rho_\sigma(\mathbf{r}_\lambda) \ . \tag{18}$$

While the exact-exchange energy density exhibits a scaling of

$$e_{\mathrm{x},\sigma}^{\mathrm{ex}}(\mathbf{r}) \to \lambda^4 \cdot e_{\mathrm{x},\sigma}^{\mathrm{ex}}(\mathbf{r}_\lambda) \ , \tag{19}$$

under this transformation, the more complicated scaling of the exact correlation functional is related to the adiabatic connection.[126,129] However, in the high-density limit, i.e. $\lambda \to \infty$, simple constraints are known that can be used for the construction of new correlation functionals. In hybrid functionals in general and the LRSLH approach in particular, this concerns the additional non-local correlation term within the correlation picture (see eq. (16)). In particular, the weak scaling condition[73] requires that the exchange contribution dominates over correlation in the high-density limit

$$\lim_{\lambda\to\infty} \frac{E_{\mathrm{xc}}^{\mathrm{ex}}}{E_{\mathrm{x}}^{\mathrm{ex}}} = 1 \ . \tag{20}$$

In this case, the exact correlation energy density is thus required to scale as

$$e_{\mathrm{c}}^{\mathrm{ex}}(\mathbf{r}) \to \lambda^n \cdot e_{\mathrm{c}}^{\mathrm{ex}}(\mathbf{r}_\lambda) \ , \ n < 4 \ , \ \lambda \to \infty \ . \tag{21}$$

On the other hand, the strong scaling condition[73] requires the correlation energy to approach a constant in the high-density limit,[120,127] which results in a scaling of the exact correlation energy density of

$$e_{\mathrm{c}}^{\mathrm{ex}}(\mathbf{r}) \to \lambda^n \cdot e_{\mathrm{c}}^{\mathrm{ex}}(\mathbf{r}_\lambda) \ , \ n \leq 3 \ , \ \lambda \to \infty \ . \tag{22}$$

Naturally, satisfying the high-density limit is most relevant in regions approaching high electron densities and thus properties that sample these regions. In molecular systems, this mostly concerns core regions and core properties such as core excitations, in particular of heavy elements. In fact, even most XC functionals constructed for describing core excitations violate the high-density limit,[24,69,70,130] thus leaving significant potential for new developments to incorporate the scaling conditions.

In contrast to the iso-orbital limit (see sec. II C 1), coordinate scaling in principle affects real and inter-electronic spaces. However, the simple range-separation in RSH functionals using just a constant range-separation parameter has been shown not to be able to give the correct high-density limit. Hence, also a real-space dependence is required within the exact-exchange admixture to satisfy either of the two high-density limit conditions with respect to uniform coordinate scaling. In fact, the scaling condition can be easily implemented into the LMF and thus satisfied by LH, RSLH and

LRSLH functionals.[75] The real-space dependence in LRSH and LRSGH functionals in principle is also able to give the correct high-density limit, with the minor limitation that the additional correlation term in eq. (16) becomes fully local in the high-density limit.[73] In particular, the weak scaling condition has been considered in the recent work by Kümmel and co-worker.[71,72] However, similar to the iso-orbital constraint, satisfying either of the scaling conditions collides with the exact satisfaction of the homogeneous limit and the gradient expansion of the exchange energy density. Hence, the RSF appears to be less suited to satisfy the scaling conditions with respect to uniform coordinate scaling.

3. Asymptotic XC Potential

Another exact constraint applicable in the construction of hybrid functionals is related to the XC potential $v_{\mathrm{xc},\sigma}$, which can be defined in terms of the XC part of the Fock matrix by

$$\frac{\partial E_{\mathrm{xc}}}{\partial \mathbf{D}^{\sigma}} = \int \mathbf{X} \cdot v_{\mathrm{xc},\sigma} \cdot \mathbf{X}^{\mathrm{T}} \mathrm{d}\mathbf{r} \; . \tag{23}$$

While in KS theory the local and multiplicative XC potential is defined as functional derivative of the XC energy functional with respect to the electron density

$$v_{\mathrm{xc},\sigma}\left(\mathbf{r}\right) = \frac{\delta E_{\mathrm{xc}}}{\delta \rho_{\sigma}\left(\mathbf{r}\right)} \; , \tag{24}$$

the XC potential in GKS theory can be non-local and non-multiplicative, with KS and GKS, however, being equivalent in the case of LDA and GGA functionals. In particular, the exact asymptotic behavior of the XC potential, i.e., its behavior for infinite inter-electronic distances,[25,95,131,132]

$$v_{\mathrm{xc},\sigma}\left(\mathbf{r}\right) \xrightarrow[|\mathbf{r}-\mathbf{r}'|\to\infty]{} -\frac{1}{|\mathbf{r}-\mathbf{r}'|} \; , \tag{25}$$

can be used as exact constraint for hybrid functionals. In fact, most semi-local XC functionals feature an exponential decay of the XC potential and thus are not able to satisfy this exact constraint. On the other hand, semi-local XC functionals constructed to reproduce the correct asymptotic decay of the potential such as CAP[116,117] violate the asymptotic behavior of the XC energy density. The inability to satisfy both constraints simultaneously is a known shortcoming of semi-local functionals. On the other hand, Hartree-Fock can provide both the correct asymptotic XC potential and the correct asymptotic decay of the XC energy density. Following the reasoning, e.g., by Schmidt *et al.*,[95] the error of semi-local XC functionals can be thus interpreted as SIE of an electron interacting with its own hole upon excitation, which is the extension of the SIE on the level of the XC energy to the XC potential. In practice, providing the correct asymptotic XC potential thus has been found to be essential for the accurate description of long-range excitations in linear-response TDDFT, which mostly concerns charge-transfer excitations but in principle can also play a role for higher-lying Rydberg excitations.[11,25,52]

In view of the fact that the correct asymptotic behavior of the XC energy density needs to be sacrificed with semi-local functionals to achieve the correct asymptotic XC potential, semi-local XC functionals are considered not to be able to satisfy the the XC potential constraint. Accordingly, this is also valid for GH functionals. Schmidt *et al.* have shown that the real-space-dependent exact-exchange admixture in LHs is also not able to provide the correct asymptotic decay of the potential.[95] The simplified reasoning is as follows. While the LMF in local hybrids is a real-space-dependent ingredient and thus can be used to impose the iso-orbital limit and the correct behavior with respect to uniform coordinate scaling, the exact asymptotic behavior of the XC potential is affected by the behavior of the functional regarding the distance between an electron and its hole. Since the LMF considers just one real-space coordinate, the exact-exchange admixture in local hybrids is "blind" regarding the inter-electronic and thus the electron-hole distance. On the other hand, range-separated hybrids in all variants, including RSH, RSGH, LRSH, LRSGH, RSLH and LRSLH functionals, exhibit an explicit dependence on the inter-electronic distance through the range-separation. Hence, the correct asymptotic potential can be ensured as long as 100% exact exchange is employed in the long range. Beyond that, the asymptotic potential does not provide further constrictions regarding the exact-exchange admixture, neither on the RSF nor on the LMF.

4. Homogeneous Limit and Gradient Expansion

When considering the formulation of LRSLH functionals in the exchange picture in eq. (3) as most general formulation for hybrid functionals on the second rung of the hybrid functional ladder, it appears reasonable to require both admixed exchange energy densities individually satisfy known exact constraints on the exchange functional. Apart from providing the correct asymptotic potential by exhibiting 100% exact exchange in the long range (see sec. II C 3), this also includes reproducing the homogeneous limit and the proper gradient expansion of the exchange energy density.[133–135] Implicitly, this also requires both exchange energy densities to scale as λ^4 with respect to uniform coordinate scaling (see eq. (19)) to ensure the correct dimensionality of the admixed energy densities. While both constraints are satisfied by the exact-exchange energy density by default, the satisfaction by $e_{\mathrm{x},\sigma}^{\mathrm{lrsh}}$ depends on the choice of the RSF and the range-separation scheme.[73] On the other hand, the choice of the LMF has no influence regarding the satisfaction of both constraints for the overall functional, since it only manages the local admixture of both exchange energy densities, so the homogeneous limit and the gradient expansion of the exchange energy density need to be satisfied for each point in real space individually.

The case of long-range exact exchange with $\omega_{\sigma} = 0$ for $e_{\mathrm{x},\sigma}^{\mathrm{lrsh}}$ is equivalent to pure semi-local exchange. Although not all semi-local exchange functionals necessarily satisfy the homogeneous limit and the gradient expansion of the exchange energy density, in principle both can be satisfied on this level.[115,120,136] Accordingly, the constraints can be satisfied by SL, GH and LH functionals. On the other hand, it could be shown that long-range exact exchange with $\omega_{\sigma} = \mathrm{const.}$, i.e., employing a conventional range-separated exchange energy density, gives a non-exchange-like scaling and is not able to provide the correct gradient expansion of the exchange energy density without setting $\omega_{\sigma} = 0$.[73] Since the latter corresponds to purely semi-local exchange, RSH, RSGH and RSLH

functionals are generally considered not to be able to satisfy the combined homogeneous limit and gradient expansion constraints. In contrast, satisfaction is generally possible with a locally-range-separated exchange energy density with long-range exact exchange.[73] While the actual form of the RSF depends on the chosen approximation for the range-separation and the order of the gradient expansion to be satisfied, the dimensionality of the RSF is basically fixed by the requirement to provide an exchange-like scaling. Accordingly, LRSH, LRSGH and LRSLH functionals are generally able to satisfy this constraints.

Apart from these general considerations, the applicability of this constraint requires a few further notes. Despite the reasonable assumption often used in the development of LMFs in the context of local hybrid functionals, employing 100% semi-local exchange in bonding regions[100] cannot be rationalized by satisfying the homogeneous limit, since exact exchange and semi-local exchange usually both satisfy the homogeneous limit. Hence, there is no difference regarding this constraint. In the context of LRSH functionals, satisfying the gradient expansion of the exchange energy density has been violated by more recent approaches by introducing an RSF scaling with $\lambda \cdot \ln(\lambda)$,[71,72] which also leads to a non-exchange-like scaling with respect to uniform coordinate scaling. In this way, the weak scaling condition with respect to uniform coordinate scaling for the additional non-local correlation energy term in eq. (16) has been satisfied without the need to introduce a proper scaling by an LMF. However, providing an exchange-like scaling within the exchange picture and satisfying the strong scaling condition in the correlation picture are two sides of the same coin that in principle need to be satisfied simultaneously. However, LRSH functionals are only able to satisfy one of both at the same time, so the necessity to choose one or the other constraint is an inherent limitation of the LRSH approach and not a shortcoming of the actual RSF model. In which cases this theoretical shortcoming poses actual problems in practice requires further assessment, since the data basis is still too small. On the other hand, within the new LRSLH approach satisfying all of the four theoretical constraints simultaneously is straightforward. In particular, the strong scaling and iso-orbital conditions can be satisfied by choosing a proper LMF model while the RSF can be chosen to provide an exchange-like-scaling $e_{\mathrm{x},\sigma}^{\mathrm{lrsh}}$ and 100% long-range exact exchange ensures the correct asymptotic XC potential.

III. EMPLOYED FUNCTIONAL MODELS

Within the new LRSLH model, there are essentially five different ingredients, that can be chosen separately, the RSF, the LMF and the CF as well as the underlying semi-local exchange and correlation functionals. However, the numerical explosion of possible combinations of these ingredients renders a comprehensive investigation of the LRSLH approach in this work impossible, in particular in comparison to the other hybrid functional models. Furthermore, satisfaction of the mentioned theoretical constraints within the existing hybrid functional approaches has not necessarily been achieved with the available ingredients thus far, even when satisfaction is possible in principle. For example, incorporating the correct scaling of the LMF together with the iso-orbital constraint is still under development. Hence, only a small number of models have been chosen for the first evaluation of the LRSLH model. To reduce the problem of over-parametrization and enabling a more reasonable assessment of the LRSLH model itself rather than the complexity of the individual ingredients, models with a small number of parameters were preferred, even if it is known that a subset of the theoretical constraints is violated.

A. Range Separation Functions

In RSH, RSGH and RSLH functionals, a constant RSF is used, i.e.,

$$\omega_\sigma^{\mathrm{c}} = c_\omega \cdot \mathrm{a}_0^{-1} \,, \tag{26}$$

with a_0 being the Bohr radius to ensure correct units and c_ω being the range separation constant. Within the LRSH, LRSGH and LRSLH approaches, three different RSF models have been investigated. The ge2-RSF

$$\omega_\sigma^{\mathrm{ge2}} = c_\omega \cdot \frac{\sqrt{5}}{18} \cdot \frac{\gamma_{\sigma\sigma}^{1/2}}{\rho_\sigma} \tag{27}$$

has been derived from the second-order gradient expansion (GE2) of the exchange energy density and thus satisfies the homogeneous limit and the gradient expansion constraints by construction if the introduced empirical parameter c_ω is set to 1.0 and Slater-Dirac exchange is used. In addition, two modified variants of the RSF model proposed by Kümmel and co-workers[72] have been employed. In the first variant, denoted as k-RSF $\omega_\sigma^{\mathrm{k}}$, the additional logarithmic term to satisfy the weak scaling condition has been removed, since its effect on atomization energies and barrier heights has been found to be rather small compared to the leading term, so the additional parameter would unnecessarily increase the complexity of the optimization problem. Hence, the k-RSF provides a proper exchange-like scaling and thus violates the scaling conditions for the additional non-local correlation term within a pure LRSH model (see sec. II C 2). In terms of the ge2-RSF, the k-RSF can be formulated as

$$\omega_\sigma^{\mathrm{k}} = \omega_\sigma^{\mathrm{ge2}} \cdot \frac{1}{1 - t_\sigma \cdot \zeta^2} \,, \tag{28}$$

where

$$t_\sigma = \frac{1}{8} \cdot \frac{\gamma_{\sigma\sigma}}{\rho_\sigma \tau_\sigma} \tag{29}$$

is the common spin-resolved meta-GGA iso-orbital indicator with the Kohn-Sham kinetic energy density τ_σ and the squared spin-density gradient

$$\gamma_{\sigma\varsigma} = \nabla^{\mathrm{T}} \rho_\sigma \cdot \nabla \rho_\varsigma \tag{30}$$

and

$$\zeta = \frac{\rho_\alpha - \rho_\beta}{\rho_\alpha + \rho_\beta} \tag{31}$$

is the spin polarization. In contrast to the original definition in the work by Kümmel and co-workers,[72] a different definition of the free parameter c_ω has been used to enable a direct comparison with the ge2-RSF. Furthermore, it should be noted that, by introducing a pole at $t_\sigma \cdot \zeta^2 = 1$, the k-RSF does not

satisfy the iso-orbital limit but just the iso-electron constraint and violates the gradient expansion condition for open-shell systems. Conceptually, the k-RSF is thus still close to its predecessor. Additionally, a modified version of the k-RSF satifying the iso-orbital limit by removing the dependence on the spin polarization has been investigated, the k0-RSF

$$\omega_\sigma^{\mathrm{k0}} = \omega_\sigma^{\mathrm{ge2}} \cdot \frac{1}{1 - t_\sigma} \,. \tag{32}$$

Both the k-RSF and the k0-RSF models have been already proposed in the original work by Brütting *et al.* for analysis reasons.[72] In summary, all three considered RSF models consist of just one parameter c_ω. A summary of further RSF models can be found in ref. 73

B. Local Mixing Functions

Apart from the constant LMF

$$g_\sigma^{\mathrm{c}} = a \,, \tag{33}$$

which is equivalent to the global exact-exchange admixture in GH, RSGH and LRSGH functionals, two further LMF models have been employed. First, this includes the common t-LMF[93,94]

$$g_\sigma^{\mathrm{ct}} = a \cdot t \tag{34}$$

with the common meta-GGA iso-orbital indicator[123,124]

$$t = \frac{1}{8} \cdot \frac{\gamma_{\alpha\alpha} + 2\gamma_{\alpha\beta} + \gamma_{\beta\beta}}{(\rho_\alpha + \rho_\beta) \cdot (\tau_\alpha + \tau_\beta)} \,. \tag{35}$$

While further LMF models satisfying more exact constraints have been proposed during the last two decades (see ref. 100 for a recent review), the common t-LMF is still among the most successful LMF models thus far, despite featuring only one parameter a. In fact, the common t-LMF violates the iso-orbital limit for $a \neq 1.0$ and the scaling constraints. However, it provides a qualitatively correct exact-exchange admixture in the different regions in real-space and thus has been used in several of the more recently developed LH functionals.[9,97] While the recently proposed LMF model by Holzer and Franzke[90] within their TMHF functional also violates these two constraints, its behavior in core regions in contrast to the t-LMF is qualitatively wrong due to almost vanishing exact-exchange contributions, despite containing more empirical parameters. For the sake of simplicity, this new LMF model thus has not been considered in this work. In analogy to the employed RSF models, an artificial spin-polarized variant of the common t-LMF, denoted as common tz-LMF,

$$g_\sigma^{\mathrm{ctz}} = a \cdot t \cdot \zeta^2 \tag{36}$$

has been used. In fact, the tz-LMF violates the iso-orbital limit even with $a = 1.0$, vanishes for all closed-shell systems and thus only satisfies the iso-electron limit. Hence, the tz-LMF is only used for analysis reasons.

C. Semi-Local Exchange and Correlation Functionals

For the construction of the different hybrid functionals, Slater-Dirac[103,104] and B88 exchange[115] have been used as semi-local exchange functionals. While in SL, GH and LH functionals the conventional full-range functionals have been employed, short-range semi-local exchange based on the Hirao approach eq. (13) is used in the remaining hybrid functional models. To ensure the correct asymptotic behavior of the XC potential, 100% exact exchange and thus 0% semi-local exchange has been used in the long range in all range-separated hybrid variants. Furthermore, the LH, RSLH and LRSLH models were constructed without considering a CF. In fact, CFs would introduce more empirical parameters that need to be optimized and potentially reduce numerical stability. Also, range-separated exchange energy densities might require the adaption of the CF models, since the currently available pig CFs are derived from full-range semi-local exchange.

Regarding the semi-local correlation functional, optimization results for five different models will be shown. Apart from LDA correlation in the PW92 parametrization,[137] this includes the GGA functional LYP[138] as well as the B95 meta-GGA functional.[139] In fact, reparametrized B95 has shown to be able to provide a sufficiently high flexibility to be successfully employed as ingredient in LH functional development. While this high flexibility would allow a higher degree of error cancellation, it could potentially disguise shortcomings of the hybrid functional model on the other hand. Hence, only the original B95 parametrization will be applied in this work, which ensures accurate opposite-spin and same-spin correlation for the helium and neon atoms, respectively, already by the semi-local correlation functional. In addition to these conventional correlation functionals, self-interaction-corrected variants of PW92 and LYP, denoted as sicPW92 and sicLYP, have been investigated. In particular, the simple self-correlation correction scheme

$$E_{\mathrm{c}}^{\mathrm{sic}} = \int \left[1 - t\left(\mathbf{r}\right) \cdot \zeta^2\left(\mathbf{r}\right)\right] \cdot e_{\mathrm{c}}\left(\mathbf{r}\right) \mathrm{d}\mathbf{r} \,, \tag{37}$$

which is used by Kümmel and co-workers in several publications, is employed.[7,71,72,75] For closed-shell molecules, the self-interaction-corrected correlation and the underlying conventional functionals are equivalent, while erroneous self-correlation is removed completely in iso-electron regions. In contrast to the constraint on hybrid exchange (see sec. II C 1), considering only the iso-electron and not the iso-orbital limit provides a more reasonable self-interaction reduction in the correlation functional, since opposite-spin correlation can be present in iso-orbital regions. In combination with LDA correlation, this simple self-interaction correction has shown surprisingly good results within certain LRSH setups,[72] so the combination with LYP can be expected to provide at least similarly good results. The additional correlation functionals PBE[120] and sicPBE as well as opposite-spin-only B95 have been only used in some test calculations on LRSH functionals but did not provide additional insight regarding the evaluation of the different hybrid functional models and are thus omitted in the analysis.

IV. COMPUTATIONAL DETAILS

All calculations in this work have been performed with a development version of the RAQET program package,[109] which has been extended by a self-consistent implementation of LRSLH functionals and the self-interaction-corrected semi-local correlation functionals in eq. (37). The former extension is based on the previously reported LH[77] and LRSH implementations[73] in the RAQET program and thus employs efficient semi-numerical integration based on the modified chain-of-spheres (mCOSX) method.[77] All calculations have been performed self-consistently using Ahlrichs-type numerical integration grids[140] of size 3 as implemented in RAQET[77] together with def2-QZVP basis sets.[141] The employed functionals are described in detail in sec. III. No dispersion correction has been added.

The different investigated hybrid functional models contain either one (GH, LH, RSH and LRSH functionals) or two empirical parameters (RSGH, RSLH, LRSGH and LRSLH functionals) that need to be optimized, while purely semi-local functionals are parameter-free. In particular, these empirical parameters were optimized with respect to the mean absolute error (MAE) regarding the AE6BH6 test set for atomization energies and transition barrier heights,[142] using the newer W4-17[143] and W4-08 reference values[144] for the AE6 and BH6 subsets, respectively. The actual parameter optimization has been performed with a Nelder-Mead simplex algorithm,[145] which is well suited for the optimization of a small number of parameters. For comparing the optimized hybrid functionals with existing XC functionals, the W4-11[18] atomization and BH76 transition barrier height test sets[22,146] have been used. While the original W4-11 reference values are used to enable comparison with literature data, updated reference values from the GMTKN55 set are used for BH76.[10]

V. RESULTS AND DISCUSSION

Since this work features the first investigation of the LRSLH model, its main goal is to provide a first assessment of the benefits of LRSLH functionals in comparison to the existing hybrid functional approaches rather than optimizing a multitude of empirical parameters within a highly complex LRSLH model. While the latter would certainly provide more potential to benefit from error compensation, it could potentially hide some of the advantages and disadvantages of the respective hybrid models. In contrast, the strategy in this work is thus to optimize the nine different hybrid functional models as described in sec. II B in different functional setups (see sec. III for details), while keeping the complexity of the ingredients responsible for the exact-exchange admixture and the number of the parameters deliberately low. Apart from enabling the investigation of a larger number of different functional setups, this also facilitates the interpretation of the results regarding the performance of the individual hybrid models.

A. Assessment of the Range Separation Function

Before turning to the investigation of the different hybrid functional models, the influence of the RSF in LRSH functionals will be revisited, since the development of suitable RSF models has gained more attention recently and the RSF is also an essential part of LRSLH functionals. As described in detail in sec. II C, the RSF in LRSH functionals in principle can satisfy the iso-orbital limit and the uniform coordinate scaling constraint on the additional non-local correlation energy but can do so only by violating the gradient expansion constraint and by giving a non-exchange-like scaling behavior of the range-separated exchange energy density.

The premise of the RSF proposed by Kümmel and coworkers[72] is to satisfy the weak scaling condition and the iso-electron limit. While the former is mainly a matter of choice between different constraints due to the restrictions of the LRSH model, which is common pratice in XC functional development, choosing the iso-electron limit over the iso-orbital limit to a large extent has been rationalized on the basis of empirical findings with LRSH functionals within a certain functional setup and the freedom of one-electron self-interaction errors. In fact, the obtained results are remarkably good, but they are in contrast to the argumentation in sec. II C 1, which strongly suggests the iso-orbital limit as constraint for hybrid functionals. To contribute to the discussion on this topic, LRSH functionals within various setups based on the four considered RSF models, including the constant range-separation parameter, the ge2-RSF, the k-RSF satisfying the iso-electron limit and the k0-RSF satisfying the iso-orbital limit, have been optimized with respect to the AE6BH6 test set. The MAEs for the different optimized one-parameter LRSH functionals can be found in table II.

TABLE II. MAE for the AE6BH6 testset in kcal/mol for different optimized LRSH functionals. Functionals have been optimized with respect to the AE6BH6 test set with different combinations of short-range semi-local exchange (X), semi-local correlation (C) and RSFs.

XC		RSF			
X	C	$\omega_\sigma^{\mathrm{c}}$	$\omega_\sigma^{\mathrm{ge2}}$	$\omega_\sigma^{\mathrm{k0}}$	$\omega_\sigma^{\mathrm{k}}$
S	PW92	6.32	4.02	26.99	27.44
	LYP	4.31	4.61	20.95	21.40
	B95	6.29	4.74	14.58	15.16
	sicPW92	32.20	24.84	22.29	2.42
	sicLYP	7.98	2.26	15.08	15.54
B88	PW92	5.03	3.88	26.49	27.34
	LYP	3.17	3.71	20.44	21.31
	B95	5.24	3.88	14.00	15.03
	sicPW92	32.20	25.60	16.80	14.95
	sicLYP	6.99	1.60	14.56	15.44

First of all, the remarkably good results found by Brütting *et al.*[72] for the combination of Slater-Dirac exchange, sicPW92 correlation and the k-RSF could be verified within the current setup, so the discrepancy between the argumentation in sec. II C 1 and the empirical findings requests further explanation. Following the argumentation that the main effect of the good performance stems from correctly addressing one-electron SIEs, one should inspect the results for three other particular combinations. When replacing the k-RSF with the k0-RSF, worse results are expected, since the stronger iso-orbital constraint is enforced. This is, in fact, the case. When replacing sicPW92 correlation with another self-interaction-

corrected semi-local correlation functional such as sicLYP, a similar performance could be expected to some extent in the case that the one-electron SIE is the most important effect. However, the combination of the k-RSF, Slater-Dirac exchange and sicLYP exhibits a much higher MAE of 15.54 kcal/mol for AE6BH6. In fact, one could argue that the self-correlation correction affects LYP in a much different way than PW92, as LYP does not cover same-spin correlation at all. Nonetheless, the contradiction is significant.

The third case concerns the replacement of Slater-Dirac exchange with B88 exchange, which can be expected to be similar for the different functional setups. However, the LRSH functional with sicPW92 correlation and the k-RSF is the only combination that exhibits a major difference between Slater-Dirac and B88 exchange. Even with a full optimization of the free parameter, the resulting MAE of 14.95 kcal/mol with B88 is one order of magnitude worse than the 2.42 kcal/mol with Slater-Dirac exchange, while in many cases the B88 results are even better, as one might expect. In fact, this suggests that the good results found in the work by Brütting *et al.* might be due to an error compensation between the RSF and the self-interaction correction just in combination with LDA exchange and correlation rather than a systematic improvement due to a correct reduction of one-electron SIEs. This is also supported by that fact that sicPW92 correlation only works well in this one case. In either case, the present data hints that further investigation is required to come to a final conclusion whether the good performance of the k-RSF in this setup is or is not just due to error compensation and thus is subject to the general zero-sum tradeoff problem of hybrid functionals.[4]

Irrespective of this special case, results obtained with the k0-RSF in either setup are consistently one order of magnitude worse than those with the best performing setups. This highlights that implementation of the iso-orbital limit into the RSF can be problematic, which supports the argument to consider the iso-orbital constraint by the LMF rather than the RSF to some extent. Among the investigated LRSH functionals, the combination of the ge2-RSF with sicLYP correlation is able to provide remarkably low errors irrespective of the chosen exchange functional, which are significantly lower than for the combination of sicPW92, Slater-Dirac exchange and the k-RSF. Without further analysis, the best available explanation for this observation thus far is an apparent fortunate error compensation between opposite-spin correlation described by sicLYP and same-spin correlation through the LRSH approach. Furthermore, it appears that the LRSH functionals with ge2-RSF usually exhibit a lower MAE than their conventional RSH counterparts. Mainly LYP seems to be an exception. Apart from that, the results for the other functional setups are unremarkable.

B. Comparison of Different Hybrid Models

Next, the performance of the different hybrid functional models will be evaluated, which includes the nine different classes up to the second rung of the hybrid functional ladder (see sec. II B for more details). In view of the findings for LRSH functionals in sec. V A, two different groups of setups have been investigated. In the first one, the special combination of Slater-Dirac exchange and sicPW92 correlation is used. In fact, this combination is mainly of interest to figure out the behavior in combination with different LMF models. Hence, the artificial common tz-LMF has been included in this group in addition to the common t-LMF. For a similar reason the k0-RSF has been included in addition to the k-RSF. MAEs for the optimized hybrid functionals can be found in table III.

TABLE III. MAE for the AE6BH6 testset in kcal/mol for different optimized hybrid functionals based on Slater-Dirac exchange and self-interaction-corrected PW92. Functionals have been optimized with respect to the AE6BH6 test set with different combinations of LMFs and RSFs.

LMF	RSF			
	–	$\omega_\sigma^{\mathrm{c}}$	$\omega_\sigma^{\mathrm{k0}}$	$\omega_\sigma^{\mathrm{k}}$
–	87.90	32.20	22.29	2.42
g_σ^{c}	32.20	32.20	22.29	2.42
g_σ^{ct}	18.70	18.70	17.25	2.42
g_σ^{ctz}	23.08	23.08	22.29	1.57

Similar to LRSH functionals, only hybrid functionals including a local range separation based on the k-RSF give reasonable results in this combination of semi-local exchange and correlation, while all other functionals with different RSF models fail to provide reasonably low errors. In particular, it should be noted that the LRSLH functional constructed using the k-RSF and the common t-LMF simply reduces to the LRSH functional with k-RSF. That is, the reasonable local exact-exchange admixture provided by the t-LMF, which has been shown to be beneficial in various local hybrid functional setups, apparently has no effect in combination with the k-RSF, so the prefactor a is simply optimized to 0.0. On the other hand, the combination of the artificial common tz-LMF with the k-RSF improves the observed MAEs. In fact, the k-RSF and the tz-LMF share the common feature to only address the iso-electron limit, so the improvement appears to be somehow systematic for the investigated properties. On the other hand, considering the qualitative violation of the iso-orbital limit by the common tz-LMF, a systematic improvement for other properties such as core excitations is questionable. However, this mainly supports the conjecture of sec. V A that the combination of sicPW92 and Slater-Dirac exchange exhibits certain systematic errors that are somehow compensated by an exact-exchange admixture considering the iso-electron limit. Regarding the performance of the LRSLH model, a definitive statement is thus not possible.

Hence, hybrid functional models based on the ge2-RSF and the common t-LMF with the different semi-local exchange and correlation functionals have been investigated in the second group. Only sicPW92 is not considered, as results turned out to be similarly bad as in LRSH functionals. MAEs of the optimized functionals for the AE6BH6 test set can be found in table IV. Without discussing all numbers in detail, a few trends can be identified. First of all, replacing the global mixing constant by an LMF, i.e., going from GH to LH, RSGH to RSLH or LRSGH to LRSLH functionals, usually improves results, except for B88 and the step from GH to LH functionals. Similarly, using a local range separation is often advantageous compared to a range separation constant, except for combinations with LYP. Despite these exceptions, either the RSLH or the LRSLH models are the best performing hybrid functional models for the respective combination of exchange and

TABLE IV. MAE for the AE6BH6 testset in kcal/mol for different optimized hybrid functionals. Functionals have been optimized with respect to the AE6BH6 test set with different combinations of semi-local exchange (S and B88), semi-local correlation (C), LMFs and RSFs. The lowest MAE for each combination of semi-local exchange and correlation functionals within a range of 0.1 kcal/mol is marked by bold type.

C	LMF	S			B88		
		–	ω_σ^c	ω_σ^{ge2}	–	ω_σ^c	ω_σ^{ge2}
PW92	–	46.42	6.32	4.02	6.93	5.03	3.88
	g_σ^c	9.08	5.78	4.02	6.93	4.89	3.88
	g_σ^{ct}	1.77	**1.48**	1.77	6.93	**3.17**	**3.16**
LYP	–	50.13	4.31	4.61	7.32	3.17	3.71
	g_σ^c	6.99	3.67	4.36	6.27	2.86	3.54
	g_σ^{ct}	4.12	**1.90**	3.87	6.74	**1.96**	3.15
B95	–	56.47	6.29	4.74	9.63	5.24	3.88
	g_σ^c	7.52	5.67	4.43	3.20	3.20	2.95
	g_σ^{ct}	4.44	**2.07**	3.44	5.06	**1.94**	2.91
sicLYP	–	56.68	7.98	2.26	9.37	6.99	1.60
	g_σ^c	7.73	5.75	2.10	1.68	1.62	1.60
	g_σ^{ct}	4.17	**1.73**	**1.67**	3.47	**1.22**	**1.30**

correlation functionals (bold font in table IV). In fact, this highlights that the wrong scaling behavior of the range separation constant is apparently negligible for the performance with respect to the investigated ground-state properties. On the other hand, RSGH and LRSGH functionals, despite also featuring two free parameters, were not able to provide similarly accurate results, which shows that considering a local exact-exchange admixture governed by an LMF is an essential part for constructing more accurate hybrid functionals. When also taking into account the satisfiability of theoretical constraints (cf. sec. II C) and the similar computation costs, the LRSLH model should be preferred over the RSLH approach.

Regarding the various combinations of semi-local exchange and correlation functionals, Slater-Dirac exchange with PW92 and B88 with sicLYP have been found to provide the best performance. While the former is known from LH functionals and is most likely due to benficial error compensation, the latter combination is rather interesting, as self-interaction-corrected LYP has not been used in any LH, LRSH or RSLH model thus far and the incorporation of GGA exchange is generally preferable. Overall, the actual performance of the different hybrid functional models varies significantly depending on the chosen semi-local exchange and correlation functionals. That is, while the benefits of the new LRSLH approach are clear in general, the effect of choosing appropriate semi-local XC ingredients might be similarly or even more important than improving the dedicated hybrid functional ingredients such as the RSF and the LMF. In principle, even fully non-local correlation would be preferable. In fact, this assessment is in line with recent LH developments focussing on the balance between different correlation effects.[9]

C. Functional Comparison

Last, the performance of the optimized hybrid functional models shall be compared with existing hybrid XC functionals from literature. For that purpose, some of the best performing optimized functionals for each hybrid functional class have been chosen. In particular, the performance with respect to the W4-11/BH76 test set is evaluated. Since both are part of the larger GMTKN55 test set, literature values are easily accessible for a large number of reference functionals. While the hybrid functionals in this work have been optimized with respect to the same properties, i.e., atomization energies and transition barrier heights, a different test set has been used for training, thus reducing the bias with respect to a potential overparametrization. The MAEs, mean signed errors (MSEs) and the optimized parameters for the chosen optimized hybrid functional models can be found in table V.

Apart from being optimized for the properties of the employed test sets, two further aspects need to be kept in mind. Due to its small size and thus low representativity, the AE6BH6 test set, despite being suited to compare the performance of the different hybrid models, is not necessarily well suited as training set for actual functional development. Furthermore, the optimized hybrid functionals contain at most two parameters. This is by far less than in some of the highly parametrized reference functionals like MN15 and M11.[147,148] In general, the shown results should be thus viewed just as a first impression to highlight the potential of LRSLH functionals.

In fact, the results obtained with the optimized LRSLH functionals are generally comparable with those of the more recently developed LH functionals. While the overall MAEs are generally lower than with the recent TMHF functional by Holzer and Franzke,[90] LH20t[9] performs slightly better, except for the LRSLH using the artificial tz-LMF and the k-RSF in its only working functional setup. Similarly, the highly parametrized Minnesota functionals fare slightly better. Only the recently developed RSLH ωLH22t[97] is able to provide a distinctly lower MAE below 2.0 kcal/mol. Interestingly, most of the optimized RSLH functionals exhibit significantly larger errors than the LRSLH models. Furthermore, the two chosen LRSLH functionals using the common t-LMF in combination with the ge2-RSF both exhibit remarkably low MSEs for both individual test sets, which indicates the potential of the LRSLH model to reduce systematic errors. Overall, the optimized hybrid models still exhibit a relatively large range regarding the exact-exchange admixture. In particular, common t-LMF prefactors range from 0.24 to 0.67 depending on the individual setup. Something similar can be observed for the RSF. In fact, there is a significant correlation between smaller LMF and larger RSF prefactors, which highlights the interdependence between the exact-exchange admixture provided by the LMF and the RSF. In general, sicLYP appears to allow the admixture of a larger amount of exact exchange, which in the context of LH functionals has been argued to be beneficial.

In essence, the proposed simple two-parameter LRSLH functionals are thus able to provide accuracies similar to some of the more accurate existing hybrid functionals. In view of the gain that appears to be possible already on the RSLH level by introducing a larger number of reasonable parameters and by improving the optimization procedure, e.g., comparing MAEs of ωLH22t with some of those of the RSLH functionals optimized in this work, significantly reduced errors can be expected for more sophisticated LRSLH functionals.

TABLE V. MAE and MSE for the W4-11 and BH76 testsets in kcal/mol for different optimized hybrid functionals categorized by the hybrid functional ladder and reference XC functionals. The LMF and RSF models together with their respective parameters a and c_ω are only given for the hybrid functionals optimized in this work.

Functional						MSE			MAE		
Type	XC	LMF	a	RSF	c_ω	W4-11	BH76	avg.	W4-11	BH76	avg.
SL	BLYP[a]	–	–	–	–	-21.46	1.85	-9.80	21.50	3.50	12.50
	SCAN[a]	–	–	–	–	-0.17	-7.36	-3.77	4.01	7.66	5.83
GH	PBE0[a]	–	–	–	–	-1.75	-3.17	-2.46	3.62	4.62	4.12
	PW6B95[a]	–	–	–	–	-0.82	-2.46	-1.64	2.43	3.81	3.12
	MN15[a]	–	–	–	–	-0.03	-1.07	-0.55	2.72	1.50	2.11
	BsicLYP	g_σ^{c}	0.30547	–	–	0.01	-1.97	-0.98	4.85	2.39	3.62
LH	LH20t[b]	–	–	–	–	-0.51	-0.99	-0.75	2.89	2.05	2.47
	TMHF[c]	–	–	–	–	-0.73	-2.71	-1.72	2.78	2.80	2.79
	SPW92	g_σ^{ct}	0.53867	–	–	0.83	-0.68	0.07	2.73	1.56	2.15
RS(G)H	LCωhPBE[a]	–	–	–	–	-3.09	0.35	-1.37	4.43	1.61	3.02
	M11[a]	–	–	–	–	-0.34	-0.67	-0.51	3.44	1.26	2.35
	BLYP	–	–	$\omega_\sigma^{\mathrm{c}}$	0.59766	-2.85	2.00	-0.42	7.61	2.70	5.16
LRSH	SsicPW92	–	–	$\omega_\sigma^{\mathrm{k}}$	1.05213	0.65	-0.34	0.16	3.29	1.80	2.54
	BsicLYP	–	–	$\omega_\sigma^{\mathrm{ge2}}$	1.33867	-0.46	-1.37	-0.92	3.14	2.01	2.58
RSLH	ωLH22t[d]	–	–	–	–	-0.68	-0.58	-0.63	2.54	1.28	1.91
	SPW92	g_σ^{ct}	0.48290	$\omega_\sigma^{\mathrm{c}}$	0.19624	0.53	-0.20	0.17	3.37	1.40	2.39
	SLYP	g_σ^{ct}	0.37289	$\omega_\sigma^{\mathrm{c}}$	0.44643	-2.52	1.39	-0.57	5.34	2.11	3.73
	BLYP	g_σ^{ct}	0.29713	$\omega_\sigma^{\mathrm{c}}$	0.41843	-2.13	0.33	-0.90	4.90	1.81	3.36
	SsicLYP	g_σ^{ct}	0.61164	$\omega_\sigma^{\mathrm{c}}$	0.33712	1.51	2.48	2.00	4.58	2.59	3.59
	BsicLYP	g_σ^{ct}	0.66611	$\omega_\sigma^{\mathrm{c}}$	0.25791	-0.76	1.69	0.47	4.26	1.98	3.12
	SB95	g_σ^{ct}	0.60635	$\omega_\sigma^{\mathrm{c}}$	0.37191	-1.96	2.58	0.31	4.91	2.83	3.87
	BB95	g_σ^{ct}	0.33799	$\omega_\sigma^{\mathrm{c}}$	0.33799	-1.79	1.81	0.01	3.86	2.18	3.02
LRSLH	SsicPW92	g_σ^{ctz}	0.25352	$\omega_\sigma^{\mathrm{k}}$	0.96734	-0.69	-1.13	-0.91	2.54	2.10	2.32
	SsicLYP	g_σ^{ct}	0.24623	$\omega_\sigma^{\mathrm{ge2}}$	1.09187	0.07	-0.59	-0.26	3.39	1.65	2.52
	BsicLYP	g_σ^{ct}	0.46732	$\omega_\sigma^{\mathrm{ge2}}$	0.91113	-0.37	-0.01	-0.19	3.83	1.39	2.61

[a] Values taken from ref. 10.
[b] Values taken from ref. 9.
[c] Values taken from ref. 90.
[d] Values taken from ref. 97.

VI. CONCLUSIONS AND OUTLOOK

In this work, I have introduced the new class of LRSLH functionals, which are a straightforward combination of LH and LRSH functionals. Apart from the formal introduction of the LRSLH model, this includes a classification of LRSLHs in comparison to existing hybrid functional classes. For that purpose, a new general classification scheme in analogy to the Jacob's Ladder of density functional approximations named as hybrid functional ladder has been proposed. By considering the dependence of the exact-exchange admixture in real and inter-electronic space on the space variables through the mixing function and RSF levels, respectively, this hybrid functional ladder defines four different rungs. While conventional GH and RSH functional are on the first rung, LH and LRSH functionals are part of the second rung. Being the most sophisticated rung-two model thus far, LRSLH functionals in principle include all other existing hybrid functional models as special cases. Additionally, four theoretical constraints that are considered to be most relevant regarding the exact-exchange admixture have been reviewed in view of LRSLH functionals, the iso-orbital limit, the high-density limit with respect to homogeneous coordinate scaling, the asymptotic behavior of the XC potential and the homogeneous limit together with the gradient expansion of the exchange energy density. In fact, the simultaneous satisfaction of these constraints within the LRSLH model is straightforward by allocating the different constraints to either the LMF, the RSF or the range separation scheme. On the other hand, other hybrid functionals even on the second rung struggle in this respect to a varying degree. The provided theoretical insights can be used as guideline for the development of new hybrid functional models.

To evaluate the performance of the new LRSLH approach in comparison to the other hybrid functionals classes on the hybrid functional ladder, different combinations of simple RSF and LMF models as well as semi-local exchange and correlation functionals have been optimized in a standard procedure with respect to atomization energies and transition barrier heights. Here, LRSLH functionals together with RSLHs have shown to be able to provide the best results of all hybrid functional models, in particular when combined with a self-interaction-corrected variant of the LYP functional and B88 exchange. In general, the functional setup has been found to have a major influence on the performance of the different hybrid functional classes, which suggests to consider this aspect to a larger extent in future studies. When applied for larger test sets, the simple two-parameter LRSLH models already provided similar performance as some of the higher-parametrized existing hybrid functional models. Despite the confirmed good performance of some functionals considering the iso-electron limit within the RSF and the LMF, the present data hints that the reason might be due to a fortunate error compensation within the specific setup based on

LDA exchange and correlation to explain the contradiction with the violation of theoretical constraints.

While the present work thus provides the theoretical background as well as a first evaluation of the LRSLH model, no functional designed for actual applications has been developed. In future work, this open aspect will be addressed by considering a more elaborated LMF model, an adequate calibration and a more elaborated optimization scheme as used, e.g., in the development of state-of-the-art local hybrid functionals. In particular, more attention will be paid to the delicate balance between different correlation effects described by the different parts of the functional.

SUPPLEMENTARY MATERIAL

The full data set of hybrid functionals optimized in this work is provided as additional .csv file. In particular, this includes the functional specifications (semi-local exchange and correlation functionals, LMF, RSF), the hybrid functional type (LH, LRSLH, etc.), the optimized LMF parameters a, the optimized RSF parameters c_ω (denoted as w in the .csv file) as well as the MAEs and MSEs in kcal/mol with respect to the AE6, BH6, W4-11 and BH76 test sets. The different LMF models are abbreviated as t (common t-LMF), c (c-LMF) and tz (common tz-LMF), while the different RSF models are abbreviated as c (c-RSF), $ge2$ (ge2-RSF), k (k-RSF) and $k0$ (k0-RSF).

ACKNOWLEDGMENTS

T.M.M. thanks Christoph Jacob for general support and Hiromi Nakai for providing access to the Raqet source code.

DATA AVAILABILITY STATEMENT

The data that supports the findings of this study are available within the article and its supplementary material.

REFERENCES

[1] A. D. Becke, "A new mixing of Hartree-Fock and local density functional theories," J. Chem. Phys. **98**, 1372–1377 (1993).
[2] W. Kohn and L. J. Sham, "Self-consistent equations including exchange and correlation effects," Phys. Rev. **140**, A1133–A1138 (1965).
[3] A. D. Becke, "Perspective: Fifty years of density-functional theory in chemical physics," J. Chem. Phys. **140**, 18A301 (2014).
[4] B. G. Janesko, "Replacing hybrid density functional theory: motivation and recent advances," Chem. Soc. Rev. **50**, 8470–8495 (2021).
[5] N. Mardirossian and M. Head-Gordon, "Thirty years of density functional theory in computational chemistry: an overview and extensive assessment of 200 density functionals," Mol. Phys. **115**, 2315–2372 (2017).
[6] A. J. Cohen, P. Mori-Sánchez, and W. Yang, "Challenges for density functional theory," Chem. Rev. **112**, 289–320 (2012).
[7] T. Schmidt and S. Kümmel, "One- and many-electron self-interaction error in local and global hybrid functionals," Phys. Rev. B **93**, 165120 (2016).
[8] K. Molawi, A. J. Cohen, and N. C. Handy, "Left–right and dynamic correlation," Int. J. Quantum Chem. **89**, 86–93 (2002).
[9] M. Haasler, T. M. Maier, R. Grotjahn, S. Gückel, A. V. Arbuznikov, and M. Kaupp, "A local hybrid functional with wide applicability and good balance between (de)localization and left-right correlation," J. Chem. Theory Comput. **16**, 5645–5657 (2020).
[10] L. Goerigk, A. Hansen, C. Bauer, S. Ehrlich, A. Najibi, and S. Grimme, "A look at the density functional theory zoo with the advanced GMTKN55 database for general main group thermochemistry, kinetics and noncovalent interactions," Phys. Chem. Chem. Phys. **19**, 32184–32215 (2017).
[11] A. D. Laurent and D. Jacquemin, "Td-dft benchmarks: A review," Int. J. Quantum Chem. **113**, 2019–2039 (2013).
[12] C. Adamo and V. Barone, "Toward reliable density functional methods without adjustable parameters: The pbe0 model," J. Phys. Chem. **110**, 6158–6170 (1999).
[13] A. D. Becke, "Densityfunctional thermochemistry. iii. the role of exact exchange," J. Chem. Phys. **98**, 5648–5652 (1993).
[14] V. N. Staroverov, G. E. Scuseria, J. Tao, and J. P. Perdew, "Comparative assessment of a new nonempirical density functional: Molecules and hydrogen-bonded complexes," J. Chem. Phys. **119**, 12129–12137 (2003).
[15] Y. Zhao and D. G. Truhlar, "The m06 suite of density functionals for main group thermochemistry, thermochemical kinetics, noncovalent interactions, excited states, and transition elements: two new functionals and systematic testing of four m06-class functionals and 12 other functionals," Theor. Chem. Account **120**, 215–241 (2008).
[16] D. Jacquemin, I. Duchemin, and X. Blase, "Is the bethe-salpeter formalism accurate for excitation energies? comparisons with tddft, caspt2, and eom-ccsd," J. Phys. Chem. Lett. **8**, 1524–1529 (2017).
[17] M. M. Zouaoui-Rabah, M. Sekkal-Rahal, F. Djilani-Kobibi, A. M. Elhorri, and M. Springborg, "Performance of hybrid dft compared to mp2 methods in calculating nonlinear optical properties of divinylpyrene derivative molecules," J. Phys. Chem. A **120**, 8843–8852 (2016).
[18] A. Karton, S. Daon, and J. M. L. Martin, "W4-11: A high-confidence benchmark dataset for computational thermochemistry derived from first-principles w4 data," Chem. Phys. Lett. **510**, 165–178 (2011).
[19] S. Klawohn, H. Bahmann, and M. Kaupp, "Implementation of molecular gradients for local hybrid density functionals using seminumerical integration techniques," J. Chem. Theory Comput. **12**, 4254–4262 (2016).
[20] A. Karton and P. R. Spackman, "Evaluation of density functional theory for a large and diverse set of organic and inorganic equilibrium structures," J. Comput. Chem. **42**, 1590–1601 (2021).
[21] M. Kaupp, H. Bahmann, and A. V. Arbuznikov, "Local hybrid functionals: An assessment for thermochemical kinetics," J. Chem. Phys. **127**, 194102 (2007).
[22] Y. Zhao, N. González-García, and D. G. Truhlar, "Benchmark database of barrier heights for heavy atom transfer, nucleophilic substitution, association, and unimolecular reactions and its use to test theoretical methods," J. Phys.Chem. A **109**, 2012–2018 (2005).
[23] T. M. Maier, H. Bahmann, A. V. Arbuznikov, and M. Kaupp, "Validation of local hybrid functionals for tddft calculations of electronic excitation energies," J. Chem. Phys. **144**, 074106 (2016).
[24] N. A. Besley, M. J. G. Peach, and D. J. Tozer, "Time-dependent density functional theory calculations of near-edge X-ray absorption fine structure with short-range corrected functionals," Phys. Chem. Chem. Phys. **11**, 10350–10358 (2009).
[25] Y. Tawada, T. Tsuneda, S. Yanagisawa, T. Yanai, and K. Hirao, "A long-range-corrected time-dependent density functional theory," J. Chem. Phys. **120**, 8425–8433 (2004).
[26] A. Dreuw, J. L. Weisman, and M. Head-Gordon, "Long-range charge-transfer excited states in time-dependent density functional theory require non-local exchange," J. Chem. Phys. **119**, 2943–2946 (2003).

[27]P. Norman and A. Dreuw, "Simulating x-ray spectroscopies and calculating core-excited states of molecules," Chem. Rev. **118**, 7208–7248 (2018).
[28]D. J. Tozer and N. C. Handy, "Improving virtual kohn–sham orbitals and eigenvalues: Application to excitation energies and static polarizabilities," J. Chem. Phys. **109**, 10180–10189 (1998).
[29]D. J. Tozer and N. C. Handy, "On the determination of excitation energies using density functional theory," Phys. Chem. Chem. Phys. **2**, 2117–2121 (2000).
[30]O. A. Vydrov and T. van Voorhis, "Nonlocal van der waals density functional: The simpler the better," J. Chem. Phys. **133**, 244103 (2010).
[31]T. Sato and H. Nakai, "Density functional method including weak interactions: Dispersion coefficients based on the local response approximation," J. Chem. Phys. **131**, 224104 (2009).
[32]T. Sato and H. Nakai, "Local response dispersion method. ii. generalized multicenter interactions," J. Chem. Phys. **133**, 194101 (2010).
[33]S. Grimme, J. Antony, S. Ehrlich, and H. Krieg, "A consistent and accurate ab initio parametrization of density functional dispersion correction (dft-d) for the 94 elements h-pu," J. Chem. Phys. **132**, 154104 (2010).
[34]S. Grimme, S. Ehrlich, and L. Goerigk, "Effect of the damping function in dispersion corrected density functional theory," J. Comput. Chem. **32**, 1456–1465 (2011).
[35]E. Caldeweyher, C. Bannwarth, and S. Grimme, "Extension of the d3 dispersion coefficient model," J. Chem. Phys. **147**, 034112 (2017).
[36]A. D. Becke and E. R. Johnson, "Exchange-hole dipole moment and the dispersion interaction revisited," J. Chem. Phys. **127**, 154108 (2007).
[37]A. D. Becke, "Real-space post-Hartree-Fock correlation models," J. Chem. Phys. **122**, 064101 (2005).
[38]A. D. Becke, "Density functionals for static, dynamical, and strong correlation," J. Chem. Phys. **138**, 074109 (2013).
[39]J. Kong and E. Proynov, "Density functional model for nondynamic and strong correlation," J. Chem. Theory Comput. **12**, 133–143 (2016).
[40]A. Mirtschink, M. Seidl, and P. Gori-Giorgi, "Energy densities in the strong-interaction limit of density functional theory," J. Chem. Theory Comput. **8**, 3097–3107 (2012).
[41]A. Seidl, A. Görling, P. Vogl, J. A. Majewski, and M. Levy, "Generalized kohn-sham schemes and the band-gap problem," Phys. Rev. B **53**, 3764–3774 (1996).
[42]J.-D. Chai, "Role of exact exchange in thermally-assisted-occupation density functional theory: A proposal of new hybrid schemes," J. Chem. Phys. **146**, 044102 (2017).
[43]H. Iikura, T. Tsuneda, T. Yanai, and K. Hirao, "A long-range correction scheme for generalized-gradient-approximation exchange functionals," J. Chem. Phys. **115**, 3540–3544 (2001).
[44]T. Tsuneda and K. Hirao, "Long-range correction for density functional theory," WIREs Comput. Mol. Sci. **120**, 375–390 (2014).
[45]A. Savin, "On degeneracy, near-degeneracy and density functional theory," in *Recent Developments and Applications of Modern Density Functional Theory*, Theoretical and Computational Chemistry, Vol. 4, edited by J. Seminario (Elsevier, 1996) pp. 327–357.
[46]A. Savin and H.-J. Flad, "Density functionals for the Yukawa electron-electron interaction," Int. J. Quantum Chem. **56**, 327–332 (1995).
[47]J. Paquier and J. Toulouse, "Four-component relativistic range-separated density-functional theory: Short-range exchange local-density approximation," J. Chem. Phys. **149**, 174110 (2018).
[48]J. Toulouse, F. Colonna, and A. Savin, "Long-range-short-range separation of the electron-electron interaction in density-functional theory," Phys. Rev. A **70**, 062505 (2004).
[49]J. Toulouse, P. Gori-Giorgi, and A. Savin, "Scaling relations, virial theorem, and energy densities for long-range and short-range density functionals," Int. J. Quantum Chem. **106**, 2026–2034 (2006).
[50]A. Savin, "Models and corrections: Range separation for electronic interaction – lessons from density functional theory," J. Chem. Phys. **153**, 160901 (2020).
[51]J. Toulouse, A. Savin, and H.-J. Flad, "Short-range exchange-correlation energy of a uniform electron gas with modified electron–electron interaction," Int. J. Quantum Chem. **100**, 1047–1056 (2004).
[52]M. J. G. Peach, P. Benfield, T. Helgaker, and D. J. Tozer, "Excitation energies in density functional theory: An evaluation and a diagnostic test," J. Chem. Phys. **128**, 044118 (2008).
[53]J. Heyd, G. E. Scuseria, and M. Ernzerhof, "Hybrid functionals based on a screened coulomb potential," J. Chem. Phys. **118**, 8207–8215 (2003).
[54]C.-W. Wang, K. Hui, and J.-D. Chai, "Short- and long-range corrected hybrid density functionals with the d3 dispersion corrections," J. Chem. Phys. **145**, 204101 (2016).
[55]T. M. Henderson, A. F. Izmaylov, and G. E. Scuseria, "The importance of middle-range hartree-fock-type exchange for hybrid density functionals," J. Chem. Phys. **127**, 221103 (2007).
[56]J.-D. Chai and M. Head-Gordon, "Systematic optimization of long-range corrected hybrid density functionals," J. Chem. Phys. **128**, 084106 (2008).
[57]J.-D. Chai and M. Head-Gordon, "Long-range corrected hybrid density functionals with damped atom–atom dispersion corrections," Phys. Chem. Chem. Phys. **10**, 6615–6620 (2008).
[58]N. Mardirossian and M. Head-Gordon, "ωxb97x-v: A 10-parameter, range-separated hybrid, generalized gradient approximation density functional with nonlocal correlation, designed by a survival-of-the-fittest strategy," Phys. Chem. Chem. Phys. **16**, 9904–9924 (2014).
[59]T. Yanai, D. P. Tew, and N. C. Handy, "A new hybrid exchange–correlation functional using the coulomb-attenuating method (cam-b3lyp)," Chem. Phys. Lett. **393**, 51–57 (2004).
[60]J.-W. Song, T. Hirosawa, T. Tsuneda, and K. Hirao, "Long-range corrected density functional calculations of chemical reactions: Redetermination of parameter," J. Chem. Phys. **126**, 154105 (2007).
[61]T. Körzdörfer, J. S. Sears, C. Sutton, and J. Brédas, "Long-range corrected hybrid functionals for π-conjugated systems: Dependence of the range-separation parameter on conjugation length," J. Chem. Phys. **135**, 204107 (2011).
[62]D. Jacquemin, B. Moore II, A. Planchat, C. Adamo, and J. Autschbach, "Performance of an optimally tuned range-separated hybrid functional for 0-0 electronic excitation energies," J. Chem. Theory Comput. **10**, 1677–1685 (2014).
[63]A. Karolewski, L. Kronik, and S. Kümmel, "Using optimally tuned range separated hybrid functionals in ground-state calculations: Consequences and caveats," J. Chem. Phys. **138**, 204115 (2013).
[64]R. Baer, E. Livshits, and U. Salzner, "Tuned range-separated hybrids in density functional theory," Annu. Rev. Phys. Chem. **61**, 85–109 (2010).
[65]Y. Imamura, R. Kobayashi, and H. Nakai, "Linearity condition for orbital energies in density functional theory (iv): Determination of range-determining parameter," Int. J. Quantum Chem. **113**, 245–251 (2013).
[66]Z. Lin and T. van Voorhis, "Triplet tuning: A novel family of non-empirical exchange-correlation functionals," J. Chem. Theory Comput. **15**, 1226–1241 (2019).
[67]A. V. Krukau, G. E. Scuseria, J. P. Perdew, and A. Savin, "Hybrid functionals with local range separation," J. Chem. Phys. **129**, 124103 (2008).
[68]S. Klawohn and H. Bahmann, "Self-consistent implementation of hybrid functionals with local range separation," J. Chem. Theory Comput. **16**, 953–963 (2020).
[69]K. Schwinn, F. Zapata, A. Levitt, E. Cancès, E. Luppi, and J. Toulouse, "Photoionization and core resonances from range-separated density-functional theory: General formalism and example of the beryllium atom," J. Chem. Phys. **156**, 224106 (2022).
[70]J. Toulouse, K. Schwinn, F. Zapata, A. Levitt, E. Cancès, and E. Luppi, "Photoionization and core resonances from range-separated time-dependent density-functional theory for open-shell states: Example of the lithium atom," J. Chem. Phys. **157**, 244104 (2023).

[71]T. Aschebrock and S. Kümmel, "Exploring local range separation: The role of spin scaling and one-electron self-interaction," J. Chem. Phys. **151**, 154108 (2019).
[72]M. Brütting, H. Bahmann, and S. Kümmel, "Hybrid functionals with local range separation: Accurate atomization energies and reaction barrier heights," J. Chem. Phys. **156**, 104109 (2022).
[73]T. M. Maier, Y. Ikabata, and H. Nakai, "Assessing locally range-separated hybrid functionals from a gradient expansion of the exchange energy density," J. Chem. Phys. **154**, 214101 (2021).
[74]J. Jaramillo, G. E. Scuseria, and M. Ernzerhof, "Local hybrid functionals," J. Chem. Phys. **118**, 1068–1073 (2003).
[75]T. Schmidt, E. Kraisler, A. Makmal, L. Kronik, and S. Kümmel, "A self-interaction-free local hybrid functional: Accurate binding energies vis-à-vis accurate ionization potentials from Kohn-Sham eigenvalues," J. Chem. Phys. **140**, 18A510 (2014).
[76]K. Burke, F. G. Cruz, and K.-C. Lam, J. Chem. Phys. **109**, 8161–8167 (1998).
[77]T. M. Maier, Y. Ikabata, and H. Nakai, "Efficient semi-numerical implementation of relativistic exact exchange within the infinite-order two-component method using a modified chain-of-spheres method," J. Chem. Theory Comput. **15**, 4745–4763 (2019).
[78]H. Bahmann and M. Kaupp, "Efficient self-consistent implementation of local hybrid functionals," J. Chem. Theory Comput. **11**, 1540–1548 (2015).
[79]F. Neese, F. Wennmohs, A. Jansen, and U. Becker, "Efficient, approximate and parallel Hartree-Fock and hybrid DFT calculations. a 'chain-of-spheres' algorithm for the Hartree-Fock exchange," Chem. Phys. **356**, 98–109 (2009).
[80]H. Laqua, T. H. Thompson, J. Kussmann, and C. Ochsenfeld, "Highly efficient, linear-scaling seminumerical exact-exchange method for graphic processing units," J. Chem. Theory Comput. **16**, 1456–1468 (2020).
[81]P. Plessow and F. Weigend, "Seminumerical calculation of the hartree–fock exchange matrix: Application to two-component procedures and efficient evaluation of local hybrid density functionals," J. Comput. Chem. **33**, 810–816 (2012).
[82]T. M. Maier, H. Bahmann, and M. Kaupp, "Efficient seminumerical implementation of global and local hybrid functionals for time-dependent density functional theory," J. Chem. Theory Comput. **11**, 4226–4237 (2015).
[83]R. Grotjahn, F. Furche, and M. Kaupp, "Development and implementation of excited-state gradients for local hybrid functionals," J. Chem. Theory Comput. **15**, 5508–5522 (2019).
[84]C. Holzer, "An improved seminumerical coulomb and exchange algorithm for properties and excited states in modern density functional theory," J. Chem. Phys. **153**, 184115 (2020).
[85]T. M. Maier, M. Haasler, A. V. Arbuznikov, and M. Kaupp, "New approaches for the calibration of exchange-energy densities in local hybrid functionals," Phys. Chem. Chem. Phys. **18**, 21133–21144 (2016).
[86]A. V. Arbuznikov and M. Kaupp, "Towards improved local hybrid functionals by calibration of exchange-energy densities," J. Chem. Phys. **141**, 204101 (2014).
[87]J. Tao, V. N. Staroverov, G. E. Scuseria, and J. P. Perdew, "Exact-exchange energy density in the gauge of a semilocal density-functional approximation," Phys. Rev. A - At. Mol. Opt. Phys. **77**, 1–9 (2008).
[88]P. de Silva and C. Corminboeuf, "Local hybrid functionals with orbital-free mixing functions and balanced elimination of self-interaction error," J. Chem. Phys. **142**, 074112 (2015).
[89]E. R. Johnson, "Local-hybrid functional based on the correlation length," J. Chem. Phys. **141**, 124120 (2014).
[90]C. Holzer and Y. F. Franzke, "A local hybrid exchange functional approximation from first principles," J. Chem. Phys. **157**, 034108 (2022).
[91]B. G. Janesko and G. E. Scuseria, "Local hybrid functionals based on density matrix products," J. Chem. Phys. **127**, 164117 (2007).
[92]B. G. Janesko and G. E. Scuseria, "Parameterized local hybrid functionals from density-matrix similarity metrics," J. Chem. Phys. **128**, 084111 (2008).
[93]H. Bahmann, A. Rodenberg, A. V. Arbuznikov, and M. Kaupp, "A thermochemically competitive local hybrid functional without gradient corrections," J. Chem. Phys. **126**, 011103 (2007).
[94]A. V. Arbuznikov and M. Kaupp, "Importance of the correlation contribution for local hybrid functionals: Range separation and self-interaction corrections," J. Chem. Phys. **136**, 014111 (2012).
[95]T. Schmidt, E. Kraisler, L. Kronik, and S. Kümmel, "One-electron self-interaction and the asymptotics of the Kohn-Sham potential: an impaired relation," Phys. Chem. Chem. Phys. **16**, 14357–14367 (2014).
[96]T. M. Henderson, B. G. Janesko, and G. E. Scuseria, "Range separation and local hybridization in density functional theory," J. Phys. Chem. A **112**, 12530–12542 (2008).
[97]S. Fürst, M. Haasler, R. Grotjahn, and M. Kaupp, "Full implementation, optimization, and evaluation of a range-separated local hybrid functional with wide accuracy for ground and excited states," J. Chem. Theory Comput. **19**, 488–502 (2023).
[98]A. Wodyński, A. V. Arbuznikov, and M. Kaupp, "Local hybrid functionals augmented by a strong-correlation model," J. Chem. Phys. **155**, 144101 (2021).
[99]A. Wodyński and M. Kaupp, "Local hybrid functional applicable to weakly and strongly correlated systems," J. Chem. Theory Comput. **18**, 6111–6123 (2022).
[100]T. M. Maier, A. V. Arbuznikov, and M. Kaupp, "Local hybrid functionals: Theory, implementation, and performance of an emerging new tool in quantum chemistry and beyond," WIREs Comput. Mol. Sci. **9**, e1378 (2019).
[101]J. P. Perdew and K. Schmidt, "Jacob's ladder of density functional approximations for the exchange-correlation energy," AIP Conf. Proc. **577**, 1–20 (2001).
[102]A. V. Arbuznikov and M. Kaupp, "Evaluation of a combination of local hybrid functionals with dft-d3 corrections for the calculation of thermochemical and kinetic data," J. Phys. Chem. A **115**, 8990–8996 (2011).
[103]J. C. Slater, "A simplification of the Hartree-Fock method," Phys. Rev. **81**, 385–390 (1951).
[104]P. A. M. Dirac, "Note on exchange phenomena in the Thomas atom," Proc. Cambridge Phil. Roy. Soc. **26**, 376–385 (1930).
[105]J. Toulouse, F. Colonna, and A. Savin, "Short-range exchange and correlation energy density functionals: Beyond the local-density approximation," J. Chem. Phys. **122**, 014110 (2005).
[106]T. M. Henderson, B. G. Janesko, and G. E. Scuseria, "Generalized gradient approximation model exchange holes for range-separated hybrids," J. Chem. Phys. **128**, 194105 (2008).
[107]J. Kirkpatrick, B. McMorrow, D. H. P. Turban, A. L. Gaunt, J. S. Spencer, A. G. D. G. Matthews, A. Obika, L. Thiry, M. Fortunato, D. Pfau, L. R. Castellanos, S. Petersen, A. W. R. Nelson, P. Kohli, P. Mori-Sánchez, D. Hassabis, and A. J. Cohen, "Pushing the frontiers of density functionals by solving the fractional electron problem," Science **374**, 1385–1389 (2021).
[108]S. G. Balasubramani, G. P. Chen, S. Coriani, M. Diedenhofen, M. S. Frank, Y. J. Franzke, F. Furche, R. Grotjahn, M. E. Harding, C. Hättig, A. Hellweg, B. Helmich-Paris, C. Holzer, U. Huniar, M. Kaupp, A. Marefat Khah, S. Karbalaei Khani, T. Müller, F. Mack, B. D. Nguyen, S. M. Parker, E. Perlt, D. Rappoport, K. Reiter, S. Roy, M. Rückert, G. Schmitz, M. Sierka, E. Tapavicza, D. P. Tew, C. van Wüllen, V. K. Voora, F. Weigend, A. Wodyński, and J. M. Yu, "Turbomole: Modular program suite for ab initio quantum-chemical and condensed-matter simulations," J. Chem. Phys. **152**, 184107 (2020).
[109]M. Hayami, J. Seino, Y. Nakajima, M. Nakano, Y. Ikabata, T. Yoshikawa, T. Oyama, K. Hiraga, S. Hirata, and H. Nakai, "RAQET: Large-scale two-component relativistic quantum chemistry program package," J. Comput. Chem. **39**, 2333–2344 (2018).
[110]B. G. Janesko, "Rung 3.5 density functionals: Another step on jacob's ladder," Int. J. Quantum Chem. **113**, 83–88 (2013).
[111]T. C. Wiles and F. R. Manby, "Wavefunction-like correlation model for use in hybrid density functionals," J. Chem. Theory Comput. **14**, 4590–4599 (2018).
[112]Z. M. Williams, T. C. Wiles, and F. R. Manby, "Accurate hybrid density functionals with uw12 correlation," J. Chem. Theory Comput. **16**, 6176–6194 (2020).
[113]J. P. Perdew, A. Ruzsinszky, J. Tao, V. N. Staroverov, and G. E. Scuseria, "Prescription for the design and selection of density functional approximations: More constraint satisfaction with fewer fits," J. Chem. Phys. **123**, 062201 (2005).

[114]J. P. Perdew, A. Ruzsinszky, J. Sun, and K. Burke, "Gedanken densities and exact constraints in density functional theory," J. Chem. Phys. **140**, 18A533 (2014).
[115]A. D. Becke, "Density-functional exchange-energy approximation with correct asymptotic behavior," Phys. Rev. A **38**, 3098–3100 (1988).
[116]J. Carmona-Espíndola, J. L. Gázquez, A. Vela, and S. B. Trickey, "Generalized gradient approximation exchange energy functional with correct asymptotic behavior of the corresponding potential," J. Chem. Phys. **142**, 054105 (2015).
[117]J. Carmona-Espíndola, J. L. Gázquez, A. Vela, and S. B. Trickey, "Global hybrid exchange energy functional with correct asymptotic behavior of the corresponding potential," Theor. Chem. Acc. **135**, 120 (2016).
[118]J. Sun, R. A., and J. P. Perdew, "Strongly constrained and appropriately normed semilocal density functional," Phys. Rev. Lett. **115**, 036402 (2015).
[119]J. W. Furness, A. D. Kaplan, J. Ning, J. P. Perdew, and J. Sun, "Accurate and numerically efficient r2scan meta-generalized gradient approximation," J. Phys. Chem. Lett. **11**, 8208–8215 (2020).
[120]J. P. Perdew, K. Burke, and M. Ernzerhof, "Generalized gradient approximation made simple," Phys. Rev. Lett. **77**, 3865–3868 (1996).
[121]E. H. Lieb and S. Oxford, "Improved lower bound on the indirect coulomb energy," Int. J. Quant. Chem. **19**, 427–439 (1981).
[122]P. Mori-Sánchez, A. J. Cohen, and W. Yang, "Discontinuous nature of the exchange-correlation functional in strongly correlated systems," Phys. Rev. Lett. **102**, 066403 (2009).
[123]J. W. Furness and J. Sun, "Enhancing the efficiency of density functionals with an improved iso-orbital indicator," Phys. Rev. B **99**, 041119(R) (2019).
[124]T. M. Maier, Y. Ikabata, and H. Nakai, "Restoring the iso-orbital limit of the kinetic energy density in relativistic density functional theory," J. Chem. Phys. **151**, 174114 (2019).
[125]D. R. Lonsdale and L. Goerigk, "The one-electron self-interaction error in 74 density functional approximations: a case study on hydrogenic mono- and dinuclear systems," Phys. Chem. Chem. Phys. **22**, 15805–15830 (2020).
[126]A. Seidl, J. P. Perdew, and M. Levy, "Strictly correlated electrons in density-functional theory," Phys. Rev. A **59**, 51–54 (1999).
[127]M. Levy, "Asymptotic coordinate scaling bound for exchange-correlation energy in density-functional theory," Int. J. Quantum Chem. **36**, 617–619 (1989).
[128]L. Calderín, "Generalization of homogeneous coordinate scaling in density-functional theory," Phys. Rev. A **86**, 032510 (2012).
[129]A. Görling and M. Levy, "Correlation-energy functional and its high-density limit obtained from a coupling-constant perturbation expansion," Phys. Rev. B **47**, 13105–13113 (1993).
[130]Y. Jin and R. J. Bartlett, "Accurate computation of x-ray absorption spectra with ionization potential optimized global hybrid functional," J. Chem. Phys. **149**, 064111 (2018).
[131]C.-O. Almbladh and A. C. Pedroza, "Density-functional exchange-correlation potentials and orbital eigenvalues for light atoms," Phys. Rev. A **29**, 2322–2330 (1984).
[132]M. Levy, J. P. Perdew, and V. Sahni, "Exact differential equation for the density and ionization energy of a many-particle system," Phys. Rev. A **30**, 2745–2748 (1984).
[133]A. D. Becke, "Hartree-fock exchange energy of an inhomogeneous electron gas," Int. J. Quantum Chem. **23**, 1915–1922 (1983).
[134]R. Wang, Y. Zhou, and M. Ernzerhof, "Fourth-order series expansion of the exchange hole," Phys. Rev. A **96**, 022502 (2017).
[135]P. S. Svendsen and U. von Barth, "Gradient expansion of the exchange energy from second-order density response theory," Phys. Rev. B **54**, 17402–17413 (1996).
[136]J. P. Perdew, J. Tao, V. N. Staroverov, and G. E. Scuseria, "Meta-generalized gradient approximation: Explanation of a realistic nonempirical density functional," J. Chem. Phys. **120**, 6898–6911 (2004).
[137]J. P. Perdew and Y. Wang, "Accurate and simple analytic representation of the electron-gas correlation energy," Phys. Rev. B **45**, 13244–13249 (1992).
[138]C. Lee, W. Yang, and R. G. Parr, "Development of the Colle-Salvetti correlation-energy formula into a functional of the electron density," Phys. Rev. B **37**, 785–789 (1988).
[139]A. D. Becke, "Density-functional thermochemistry. iv. a new dynamical correlation functional and implications for exact-exchange mixing," J. Chem. Phys. **104**, 1040–1046 (1996).
[140]O. Treutler and R. Ahlrichs, "Efficient molecular numerical integration schemes," J. Chem. Phys. **102**, 346–354 (1995).
[141]F. Weigend and R. Ahlrichs, "Balanced basis sets of split valence, triple zeta valence and quadruple zeta valence quality for h to rn: Design and assessment of accuracy," Phys. Chem. Chem. Phys. **7**, 3297–3305 (2005).
[142]B. J. Lynch and D. G. Truhlar, "Small representative benchmarks for thermochemical calculations," J. Phys. Chem. A **107**, 8996–8999 (2003).
[143]A. Karton, N. Sylvetsky, and J. M. L. Martin, "W4-17: A diverse and high-confidence dataset of atomization energies for benchmarking high-level electronic structure methods," J. Comput. Chem. **38**, 2063–2075 (2017).
[144]A. Karton, A. Tarnopolsky, J. F. Lamère, G. C. Schatz, and J. M. L. Martin, "Highly accurate first-principles benchmark data sets for the parametrization and validation of density functional and other approximate methods. derivation of a robust, generally applicable, double-hybrid functional for thermochemistry and thermochemical kinetics," J. Chem. Phys. **112**, 12868–12886 (2008).
[145]J. A. Nelder and R. Mead, "A simplex method for function minimization," The Computer Journal **7**, 308–313 (1965).
[146]Y. Zhao, B. J. Lynch, and D. G. Truhlar, "Multi-coefficient extrapolated density functional theory for thermochemistry and thermochemical kinetics," Phys. Chem. Chem. Phys. **7**, 43–52 (2005).
[147]R. Peverati and D. G. Truhlar, "Improving the accuracy of hybrid meta-gga density functionals by range separation," J. Phys. Chem. Lett. **2**, 2810–2817 (2011).
[148]H. S. Yu, X. He, S. L. Li, and D. G. Truhlar, "Mn15: A kohn–sham global-hybrid exchange–correlation density functional with broad accuracy for multi-reference and single-reference systems and noncovalent interactions," Chem. Sci. **7**, 5032–5051 (2015).